Physics modelling for the measurement of the W-boson mass with ATLAS

Stefano Camarda

W-boson mass topical meeting
CERN – 22 Jun 2017

Physics modelling for the W mass measurement

- Introduction
- Physics modelling overview
- QCD corrections
  - Transverse momentum
  - Rapidity
  - Angular coefficients
- Electroweak corrections
- Summary and prospects

(QCD corrections:)
- *What was done*
- *What we wish to do*

W mass at the LHC

A proton-proton collider is the most challenging enviroment to measure m_W, worse compared to e+e- and proton-antiproton

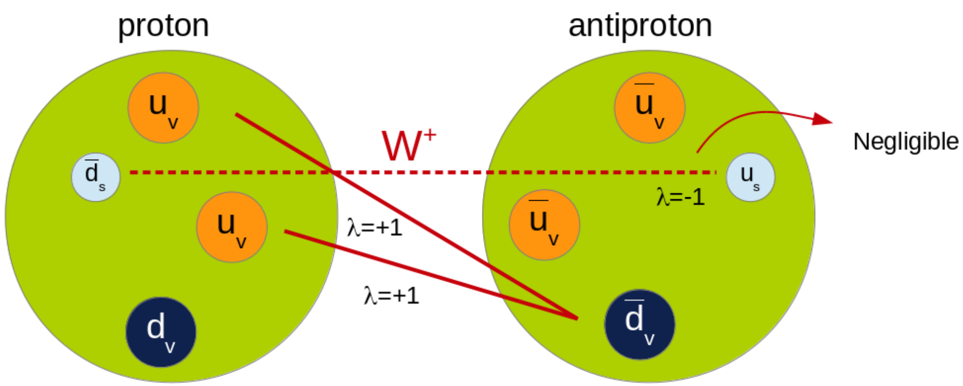

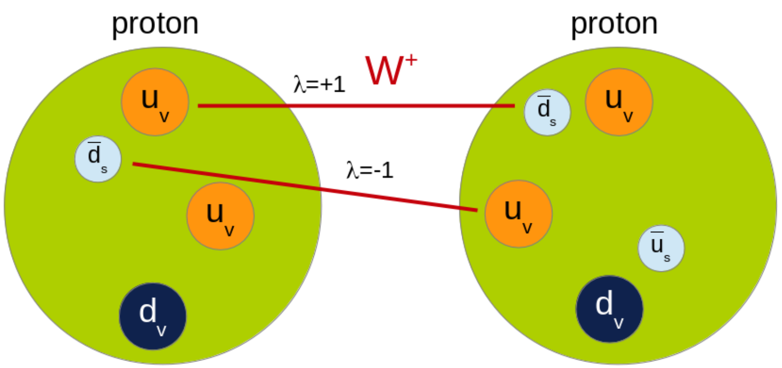

In $p\bar{p}$ collisions W bosons are mostly produced in the same helicity state

In pp collisions they are equally distributed between positive and negative helicity states

Large PDF-induced W-polarisation uncertainty affecting the p_T lepton distribution

Further QCD complications

- Heavy-flavour-initiated processes
- W+, W- and Z are produced by different light flavour fractions
- Larger gluon-induced W production

Larger Z samples, available for detector calibration given the precisely known Z mass → most of the measurement is then the transfer from Z to W

Physics modelling for the W mass measurement

The ATLAS result equals in precision the previous single-experiment best measurement of CDF

$$M_W = 80369.5 \pm 18.5 \text{ MeV}$$

arXiv:1701.07240

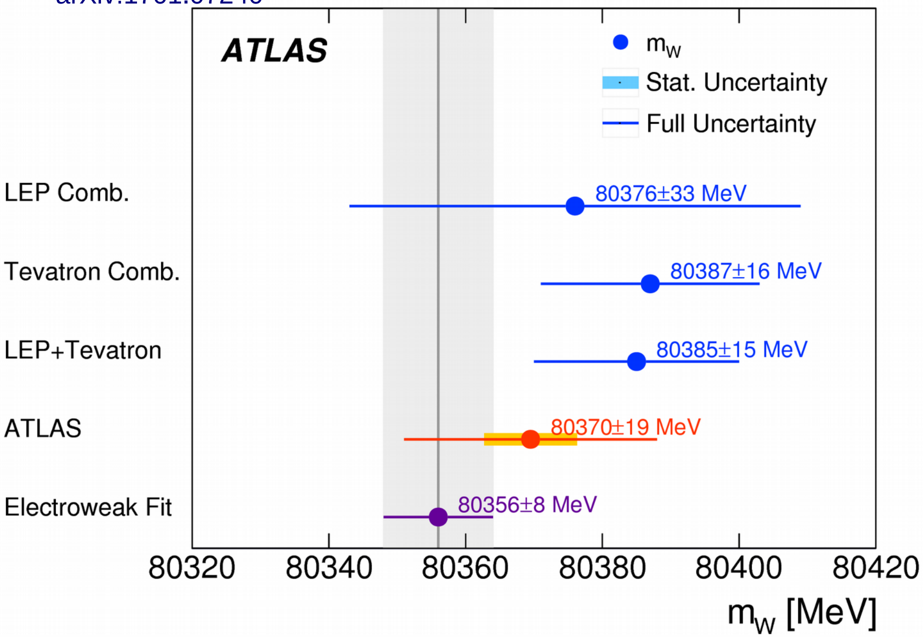

$$M_W = 80369.5 \pm 6.8 \text{ (stat)} \pm 10.6 \text{ (exp.syst.)} \pm 13.6 \text{ (model.syst.) MeV}$$

The dominant uncertainty is due to the physics modelling...

Combined categories	Value [MeV]	Stat. Unc.	Muon Unc.	Elec. Unc.	Recoil Unc.	Bckg. Unc.	QCD Unc.	EW Unc.	PDF Unc.	Total Unc.	χ^2/dof of Comb.
m_T-p_T^ℓ, $W^\pm$, e-μ	80369.5	6.8	6.6	6.4	2.9	4.5	8.3	5.5	9.2	18.5	29/27

...and the largest contributions are from QCD

Physics modelling strategy

- Start from a Powheg+Pythia 8 fully simulated MC sample
- Apply the dominant QED FSR corrections, treat the rest of EW corrections as uncertainties
- For QCD corrections, factorize the fully differential leptonic Drell-Yan cross section in various terms, and use the most appropriate model for each of them
- Use ancillary measurements of Drell-Yan processes to:
  - Fit the parameters of the model
  - Validate the model
  - Assess the uncertainties
- Use Z mass fits and W control plots to further validate the modelling and cross check the uncertainties
- Use the compatibility of W mass categories to further validate the modelling

Overview of physics modelling corrections

- QCD corrections
  - Transverse momentum distribution
  - Rapidity differential cross section
  - Angular coefficients

- Electroweak corrections
  - QED FSR and ISR
  - Running width in the Breit-Wigner parametrisation
  - Pure virtual EW (treated as unc.)
  - FSR $\gamma^* \rightarrow ll$ pair production (treated as unc.)

Physics modeling

$$\frac{d\sigma}{dp_1\,dp_2} = \left[\frac{d\sigma(m)}{dm}\right]\left[\frac{d\sigma(y)}{dy}\right]\left[\frac{d\sigma(p_T, y)}{dp_T\,dy}\left(\frac{d\sigma(y)}{dy}\right)^{-1}\right]\left[(1+\cos^2\theta) + \sum_{i=0}^{7} A_i(p_T, y)P_i(\cos\theta, \phi)\right]$$

Breit-Wigner

NNLO pQCD

Parton Shower

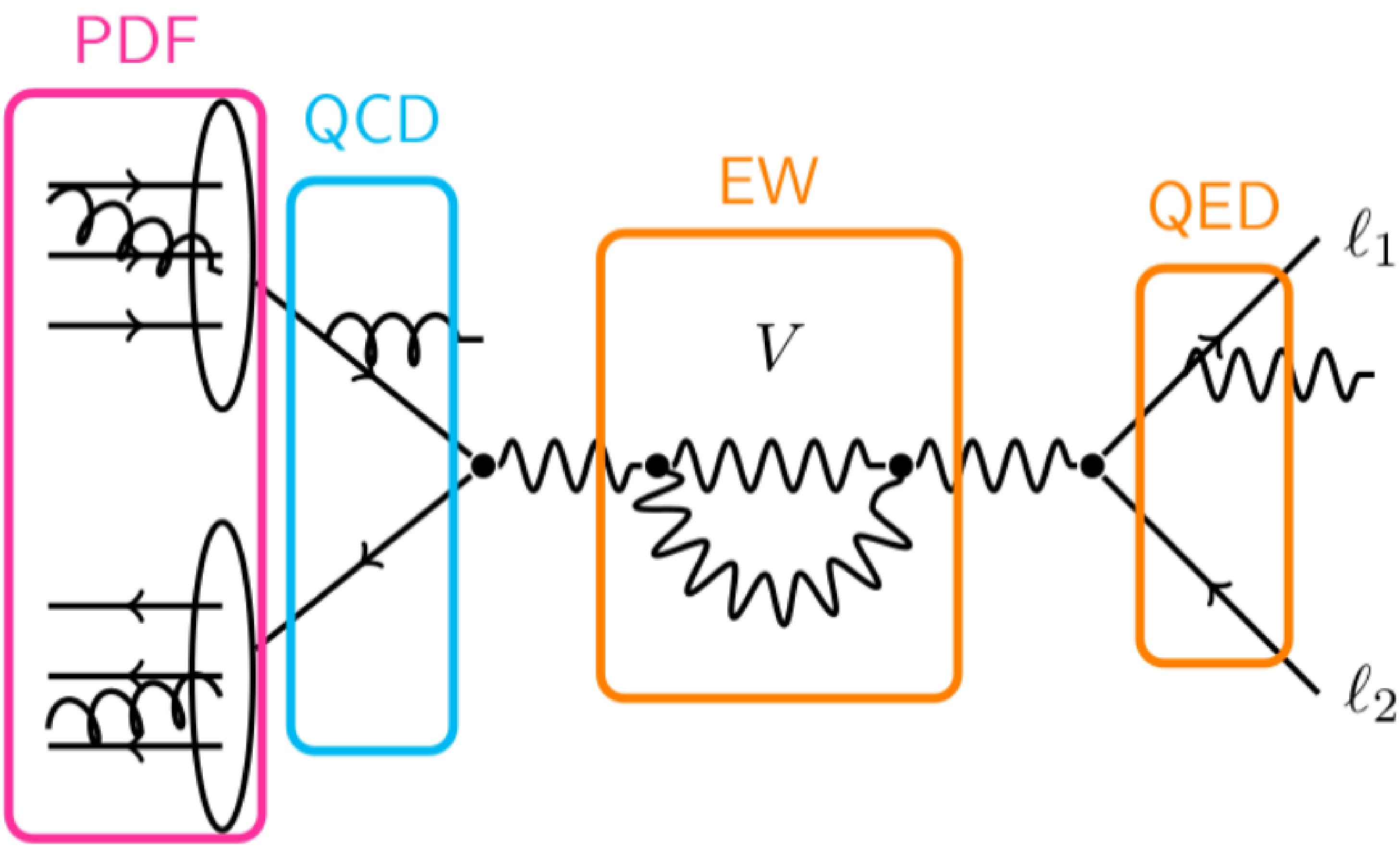

QCD corrections overview

- Inspired by this decomposition, we used an approximation of it

$$\frac{d\sigma}{dp_1\,dp_2} = \left[\frac{d\sigma(m)}{dm}\right]\left[\frac{d\sigma(y)}{dy}\right]\left[\frac{d\sigma(p_T, y)}{dp_T\,dy}\left(\frac{d\sigma(y)}{dy}\right)^{-1}\right]\left[(1+\cos^2\theta) + \sum_{i=0}^{7} A_i(p_T, y) P_i(\cos\theta, \phi)\right]$$

Breit-Wigner

NNLO pQCD

Parton Shower

- Each of the four terms is modelled with the model which is most appropriate and in best agreement with the data
  - The dσ/dm is modelled with a Breit-Wigner parametrisation
  - The dσ/dy and the Ai coefficients are modelled with fixed order pQCD at NNLO
  - The dσ/dpt is modelled with parton shower or analytic resummation

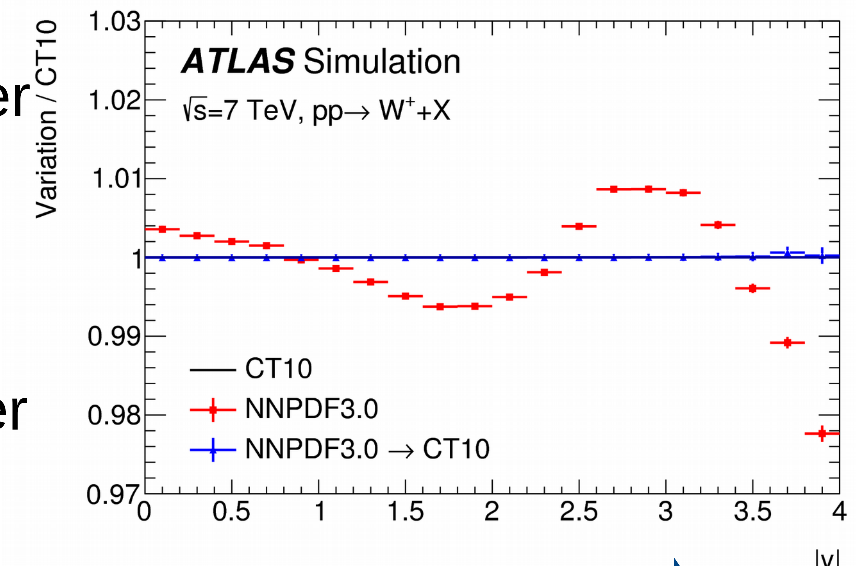

- The validity of the approximate decomposition was checked by reweighting model A to model B, and comparing to the orginal model B. The test showed no bias on m_W within 2 MeV of stat uncertainty

Physics modelling – DY ancillary measurements

$$\frac{d\sigma}{dp_1\,dp_2} = \left[\frac{d\sigma(m)}{dm}\right]\left[\frac{d\sigma(y)}{dy}\right]\left[\frac{d\sigma(p_T,y)}{dp_T\,dy}\left(\frac{d\sigma(y)}{dy}\right)^{-1}\right]\left[(1+\cos^2\theta)+\sum_{i=0}^{7}A_i(p_T,y)P_i(\cos\theta,\phi)\right]$$

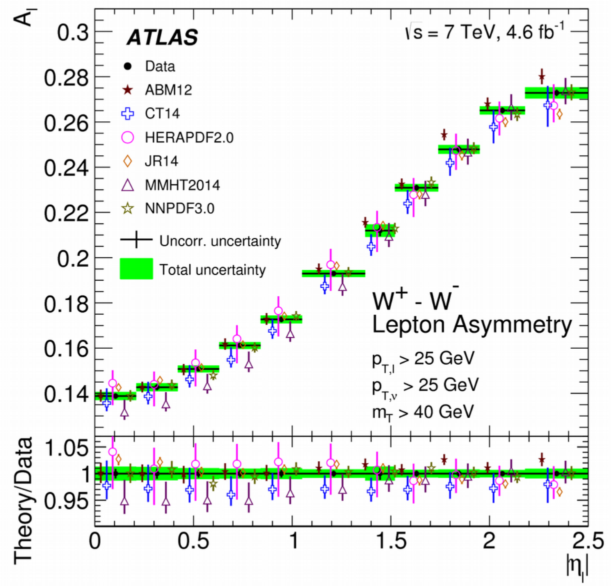

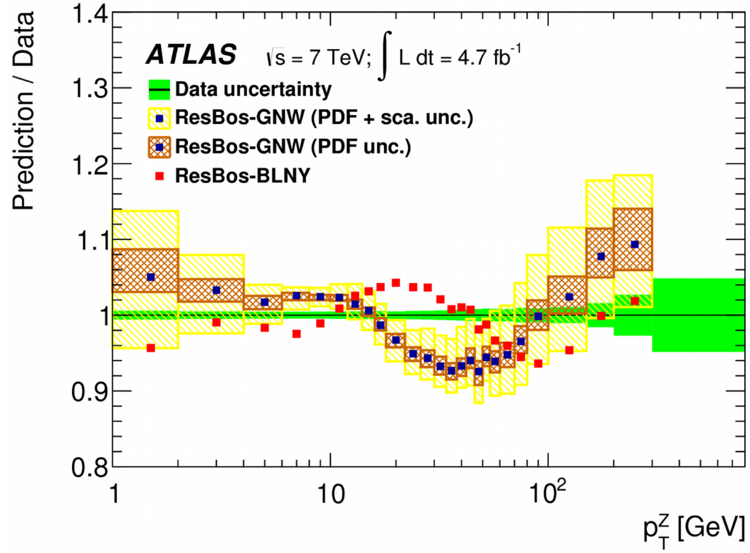

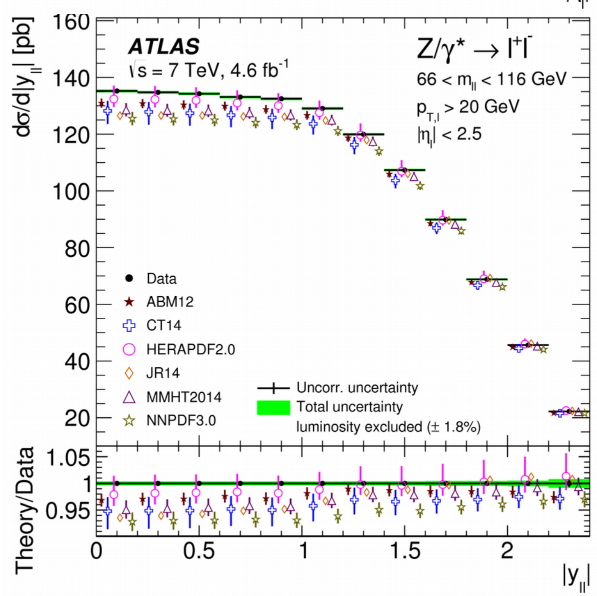

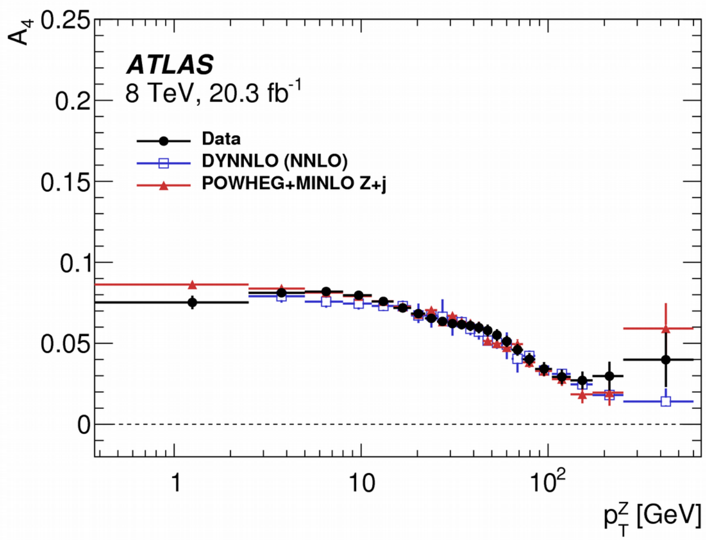

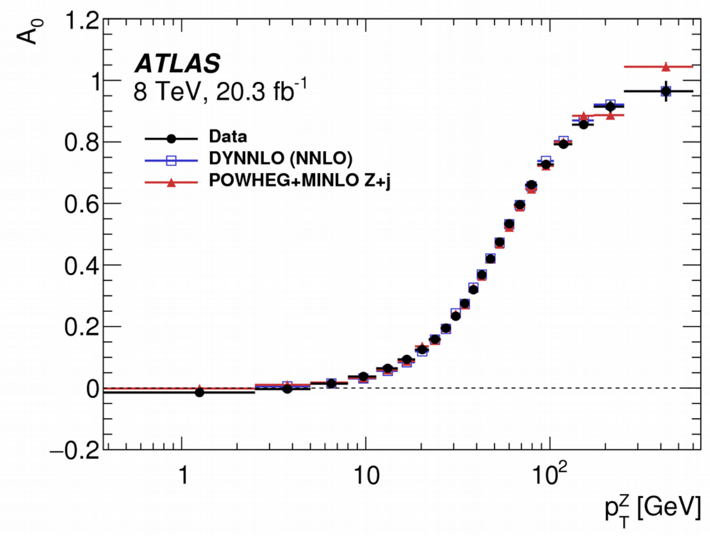

Physics modelling p_T W – Pythia 8 AZ tune

- Pythia8 AZ tune is a fit to the p_T Z measurement at 7 TeV

	PYTHIA8
Tune Name	AZ
Primordial k_T [GeV]	1.71 ± 0.03
ISR $\alpha_S^{ISR}(m_Z)$	0.1237 ± 0.0002
ISR cut-off [GeV]	0.59 ± 0.08
χ^2_{min}/dof	$45.4/32$

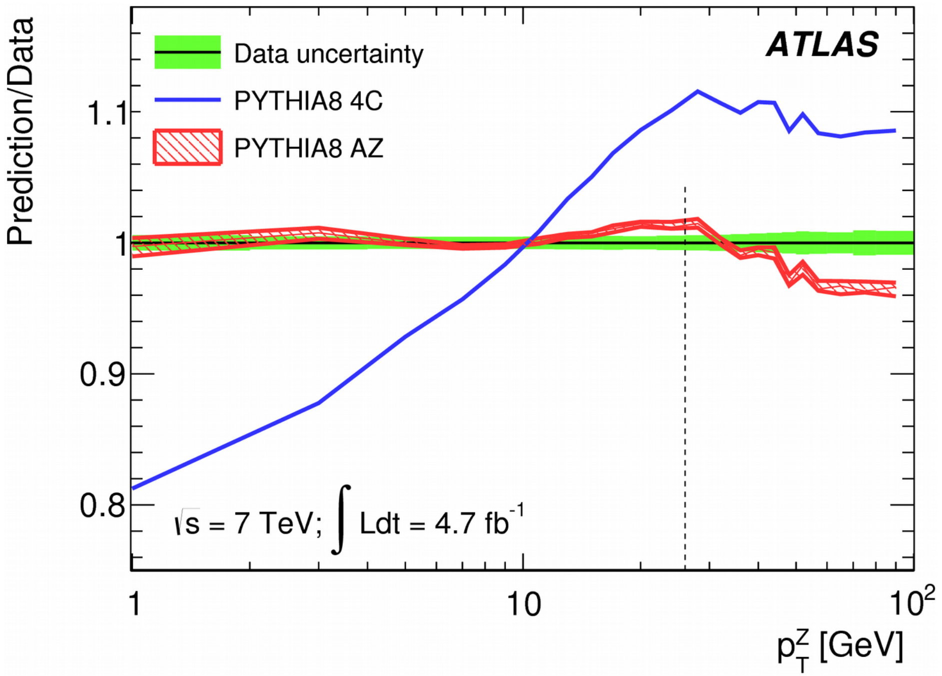

- The Pythia8 AZ tune describe the p_T Z data within 2% inclusively and in rapidity bins
- Pythia8 is used to predict the p_T W distribution and to evaluate uncertainties on p_T W

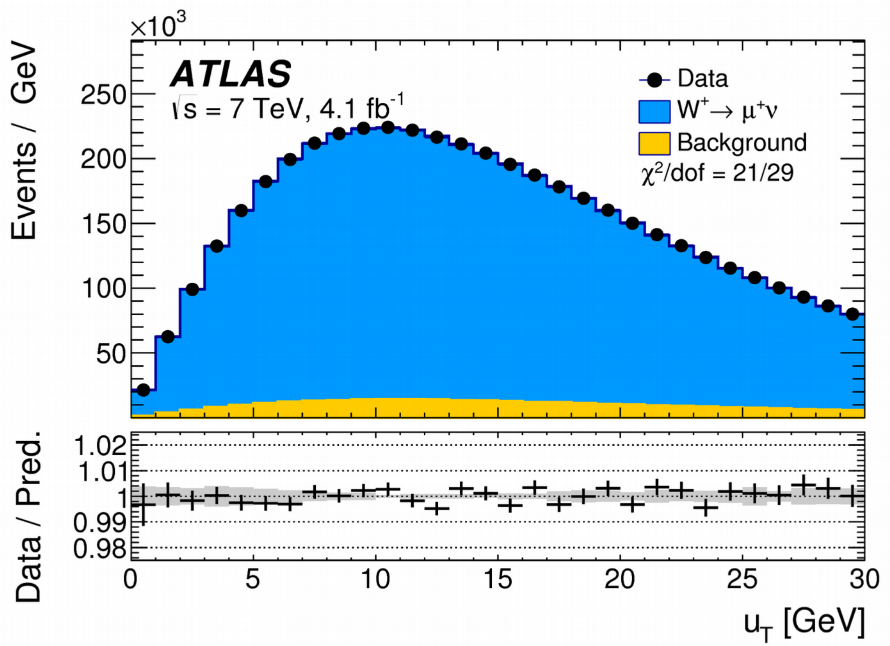

Uncertainties in the p_T W modeling

- Heavy-flavour-initiated (HFI) production introduce differences between Z and W production
- HFI production determines a harder boson p_T spectrum, $cc \rightarrow Z$ and $bb \rightarrow Z$ are 6% and 3% of Z production, $cs \rightarrow W$ is ~20% of W production
- HFI addressed with charm-quark mass variations, and by decorrelating the PS μ_F between light and HFI processes

p_T W theory uncertainties are evaluated as the sum of experimental Z p_T unc. and theory unc. on the W/Z p_T ratio

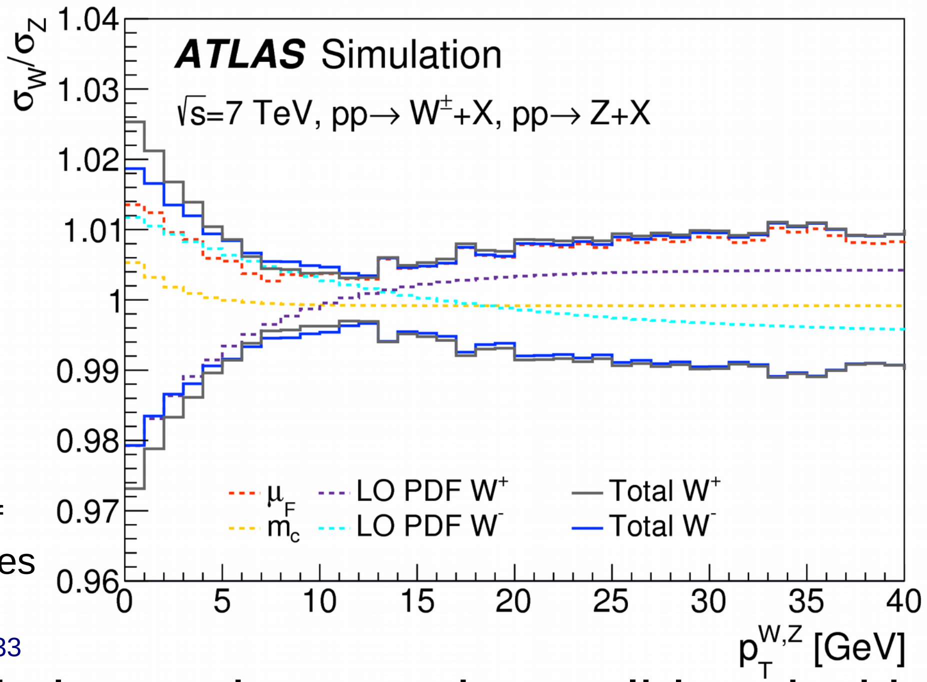

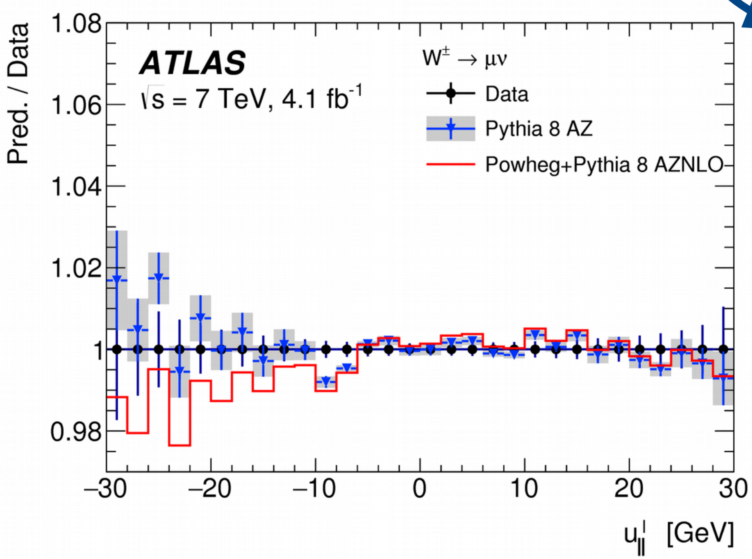

This procedure is a proxy for variations of the HF matching scales in the PDFs, see arXiv:1605.01733

Central prediction and uncertainty validated with the recoil distribution → when using the data to constrain the model we end up with compatible central value and similar uncertainties

Higher order models for p_T W

Since the p_T Z distribution is very well measured, for us it is relevant to discuss theoretical uncertainties on the W/Z p_T distribution

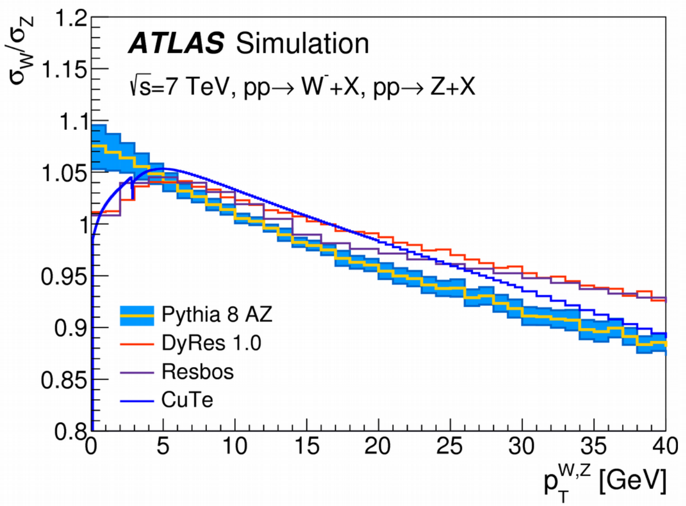

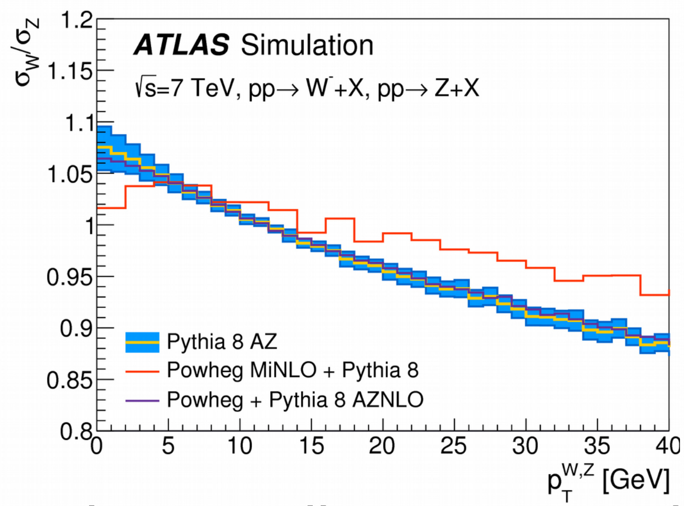

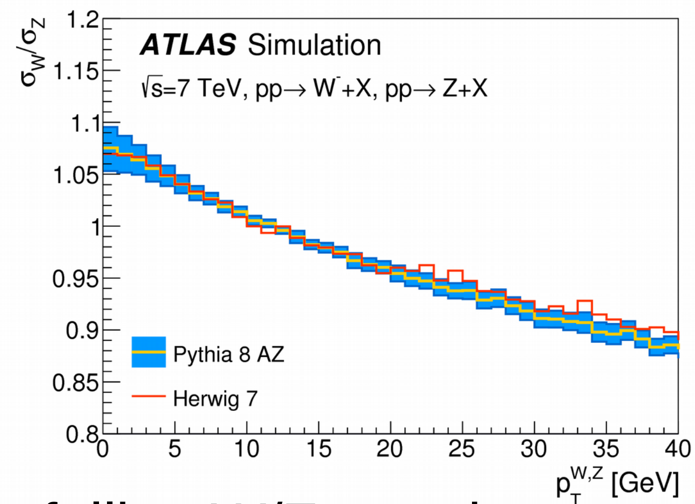

Only Herwig, Pythia, and Powheg predict a monotonic falling W/Z pt ratio

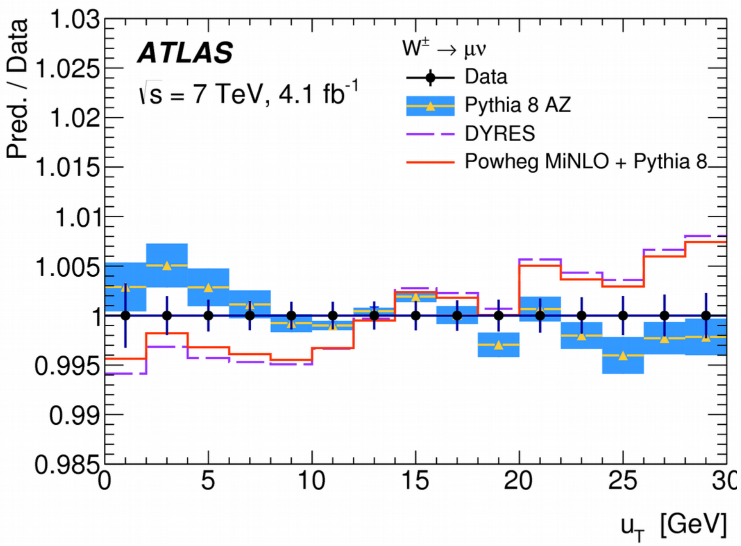

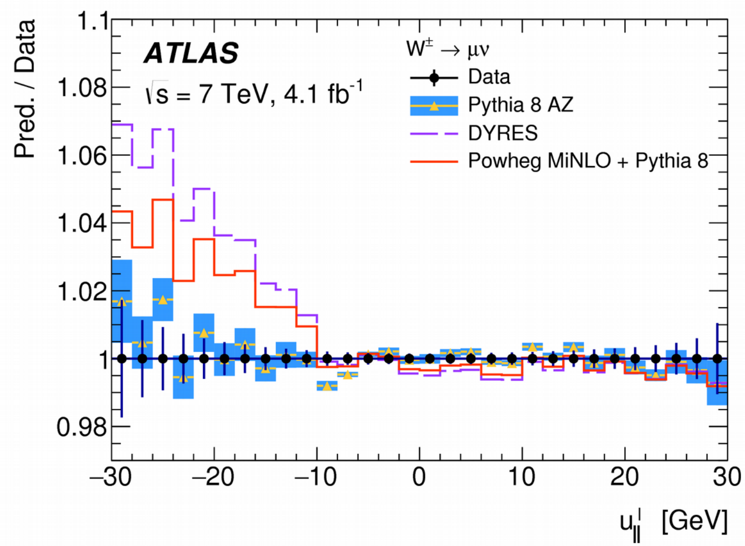

We would like to move to NNLL predictions, but currently they are strongly disfavoured by the data.
→ *Why?*

Missing QCD higher orders for the W/Z p_T ratio

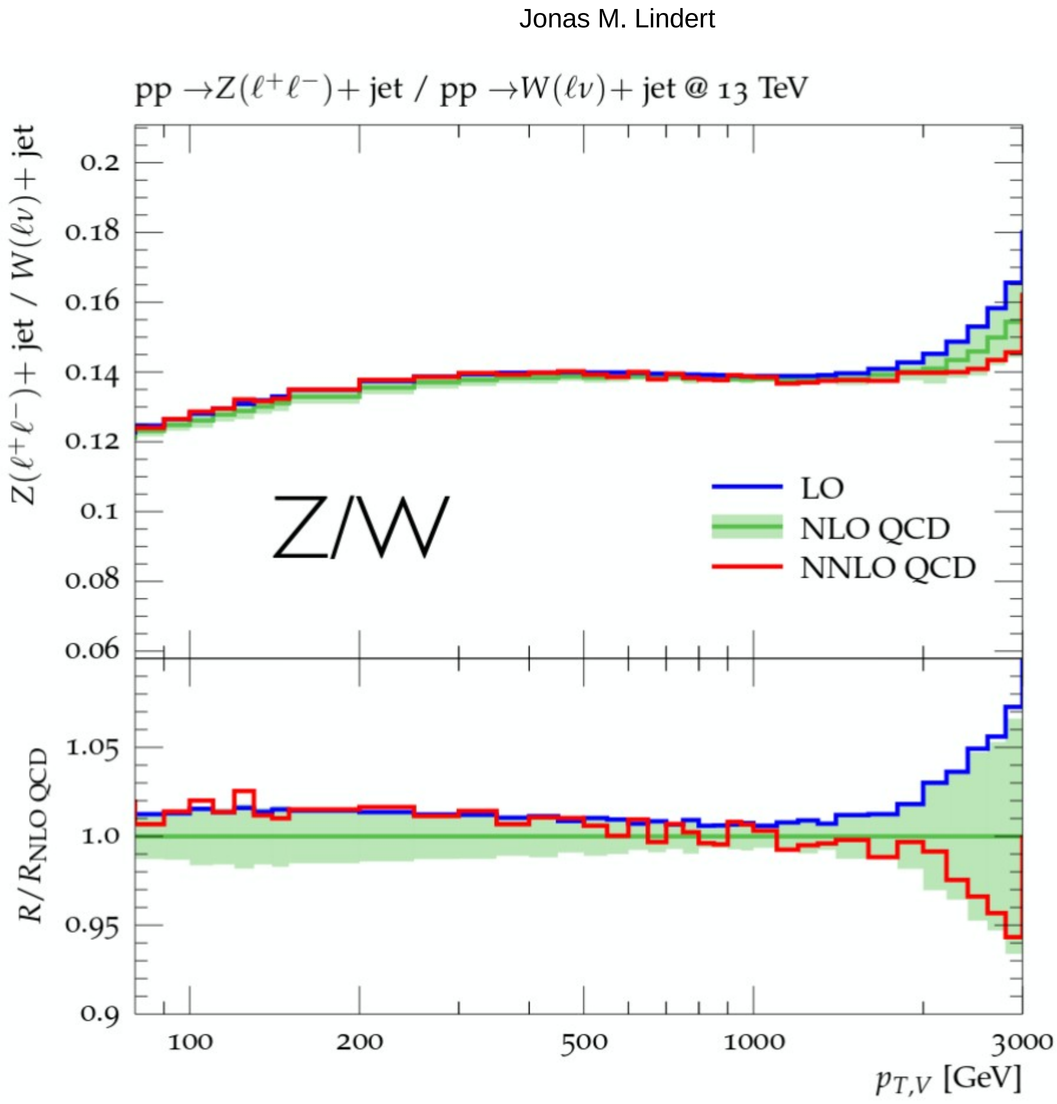

- Good convergence of the perturbative QCD series for the W/Z p_T ratio above 30 GeV

  What about < 30 GeV? Is it possible to do a similar analysis with LL, NLL, NNLL predictions?

Missing pQCD higher orders for the W/Z p_T ratio

Fred Olness

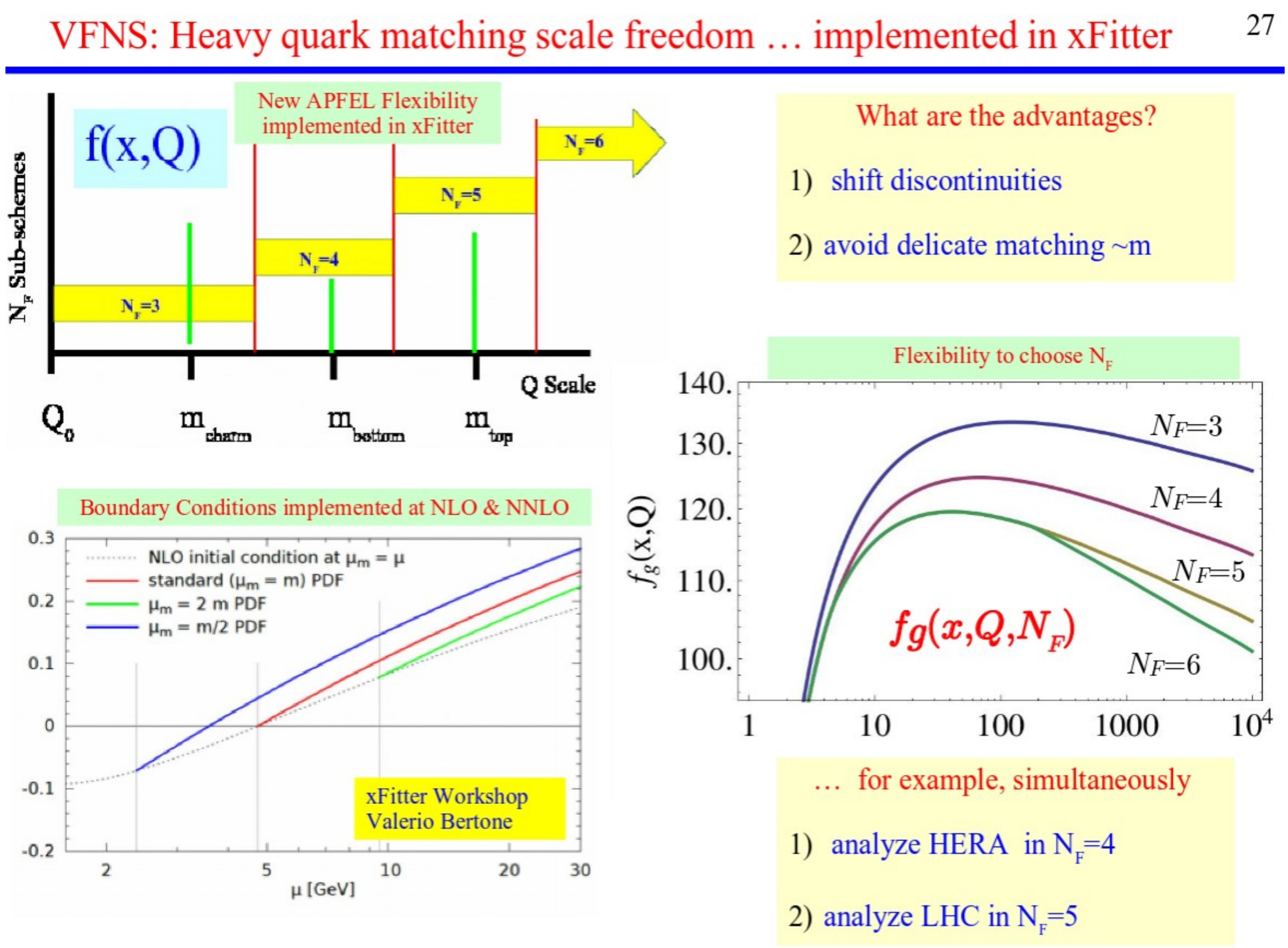

- APFEL and xFitter now allows varying the HF matching scales

Is this a better way to address HF uncertainties?

Alternative path: measure p_T W

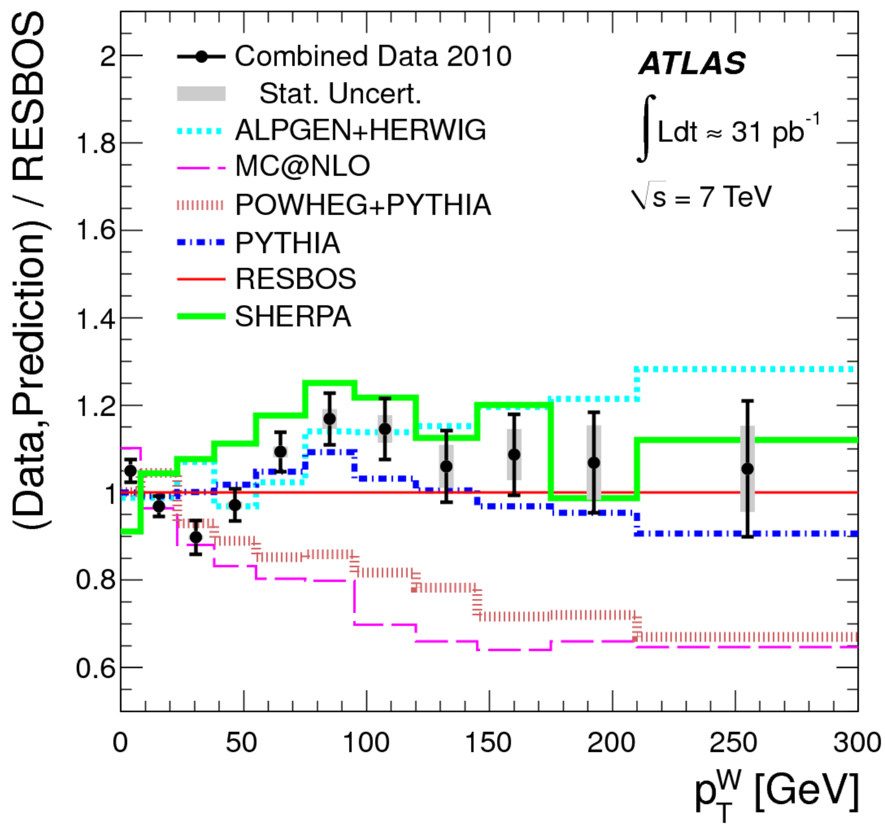

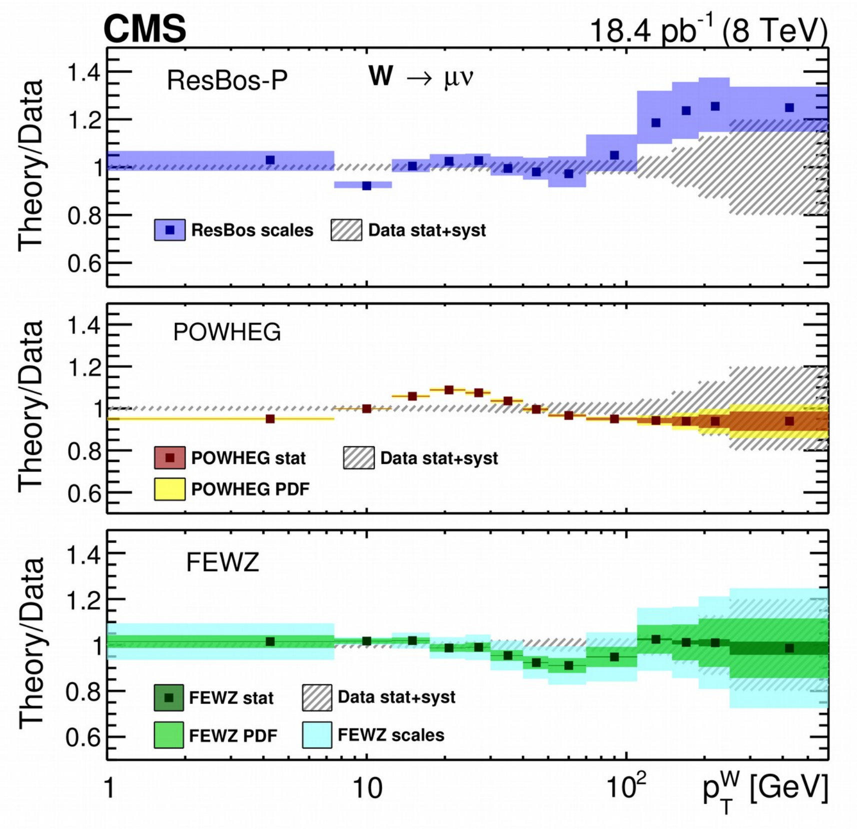

- Need approximately 1% uncertainty with bins < 5 GeV
- May be possible with a low pileup run
- Hopefully provide important input for theorists

Physics modelling – Rapidity distributions

- Rapidity distributions are modeled with NNLO predictions
- Following the strong indication of unsuppressed strangeness from the W, Z rapidity data, the CT10nnlo PDF is used, which is in good agreement with data thanks to its milder strangeness suppresion.

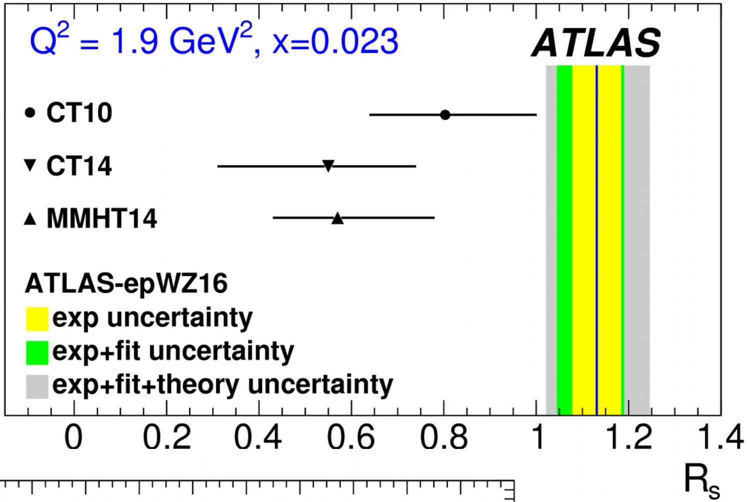

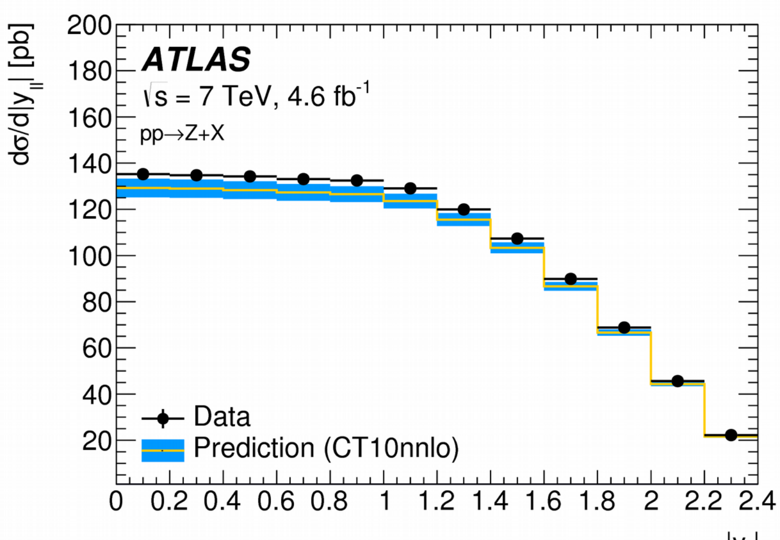

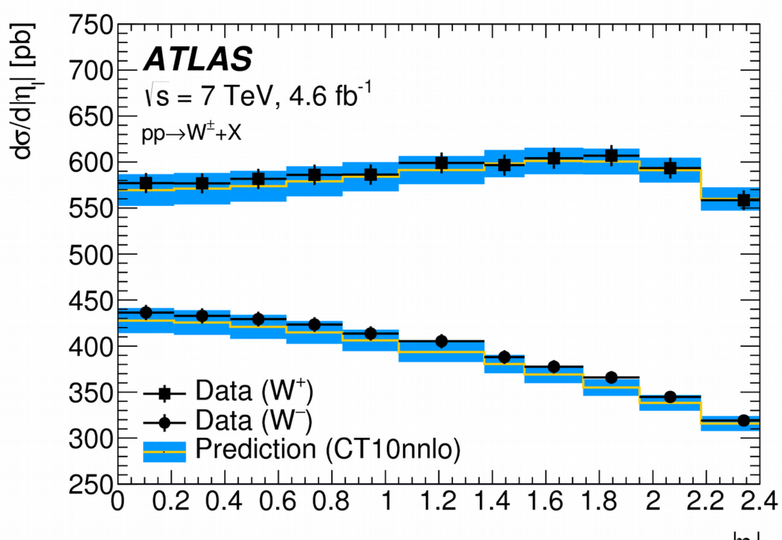

- CT14 and MMHT considered as uncertainty, other PDF sets excluded by the W, Z rapidity data
- The W, Z rapidity measurement was a crucial input to avoid a strangeness bias and reduce PDF uncertainties. However it was not directly used to derive a PDF for the mW measurement, because of large-log corrections

Physics modelling – angular coefficients A_i

- Angular coefficients are modelled with fixed order perturbative QCD at NNLO
- A fast prediction was developed, based on DYNNLO, which allows to evaluate statistically correlated PDF uncertainties

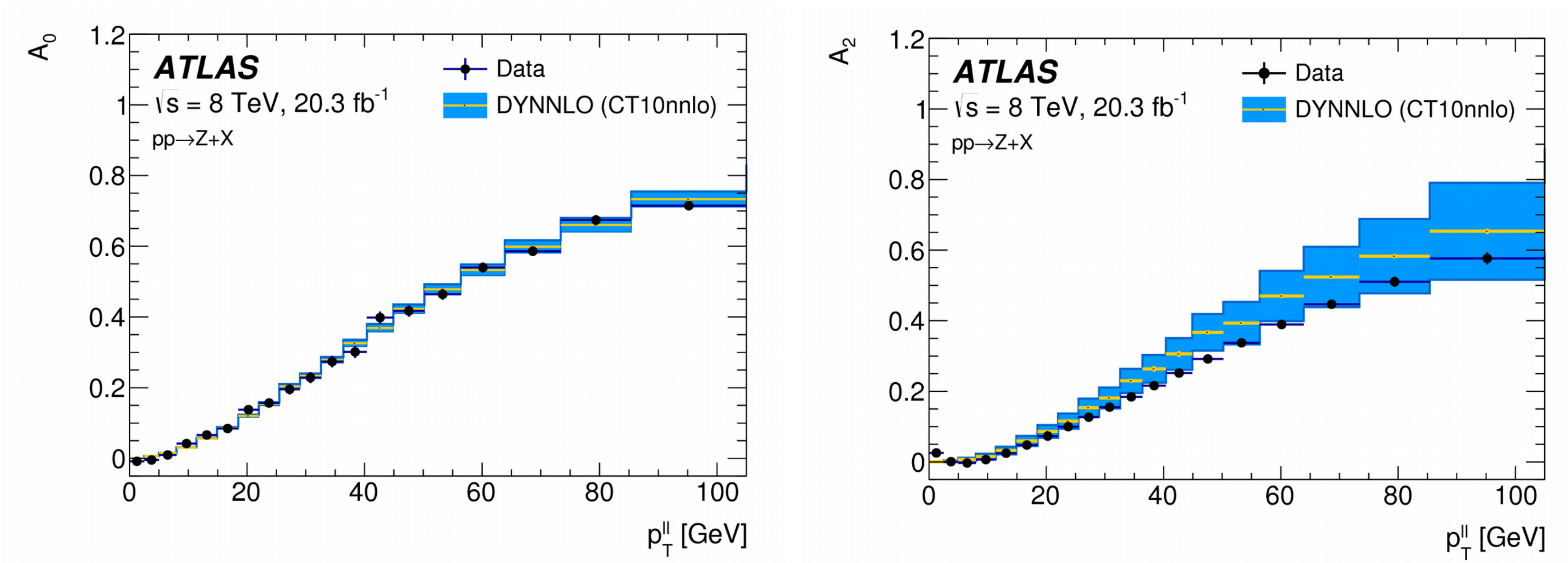

- A_i predictions are validated by comparisons to the Z measurement at 8 TeV
- Assume that pQCD is able to propagate from Z to W, since differences between W and Z in the A_i coefficients are determined by the well-known vector and axial couplings of the electroweak gauge bosons
- A_i experimental uncertainties of the Z measurement are propagated to W predictions, plus an additional uncertainty to cover A2 disagreement at high p_T

Physics modelling – angular coefficients A_i

- We have not considered the alternative approach of using theory-driven uncertainties on the QCD predictions for the angular coefficients

- In principle, nowadays it is possible to evaluate the coefficients at $O(\alpha_s^3)$ with V+jet NNLO predictions.

  Would scale variations be a sensitive approach to evaluate QCD uncertainties on the A_i? Or better use the difference between NNLO and NLO?

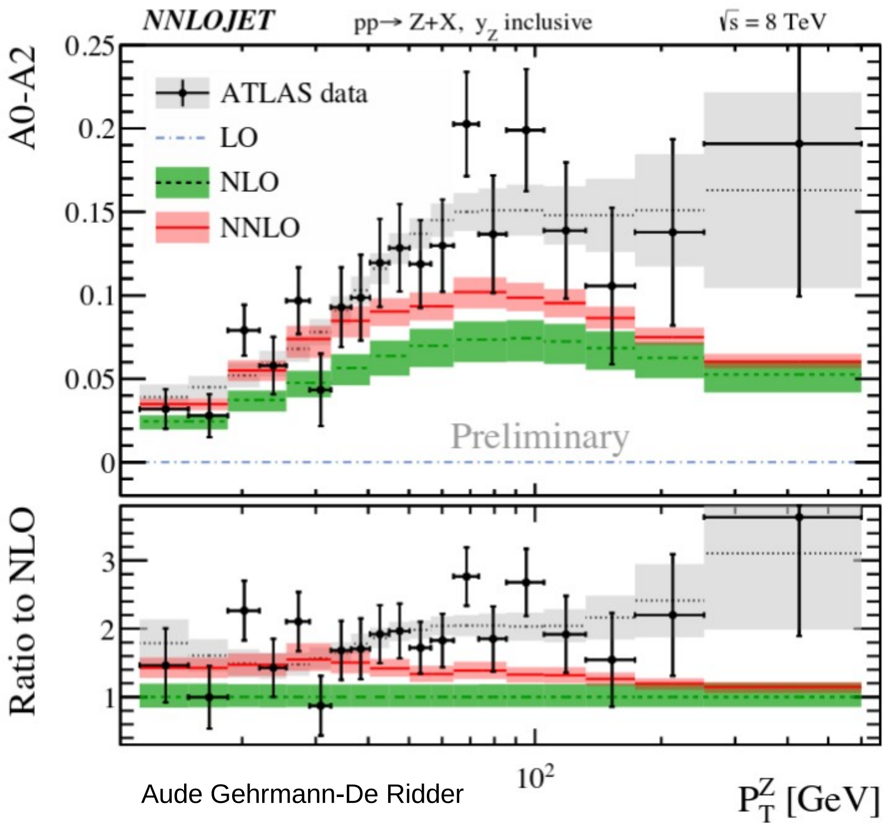

Aude Gehrmann-De Ridder

Physics modelling – angular coefficients A_i

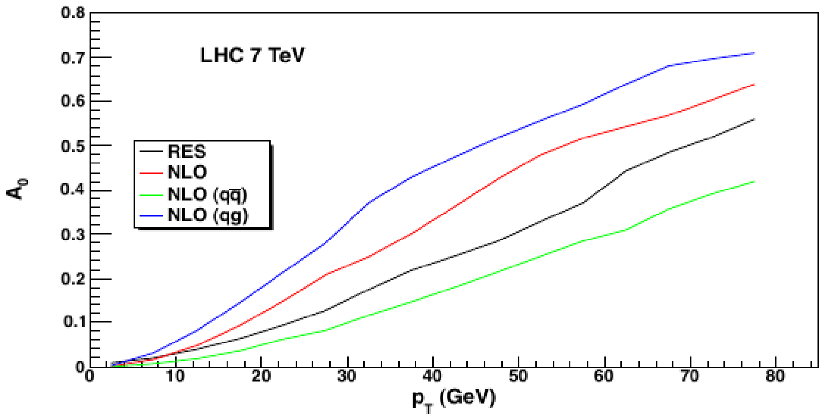

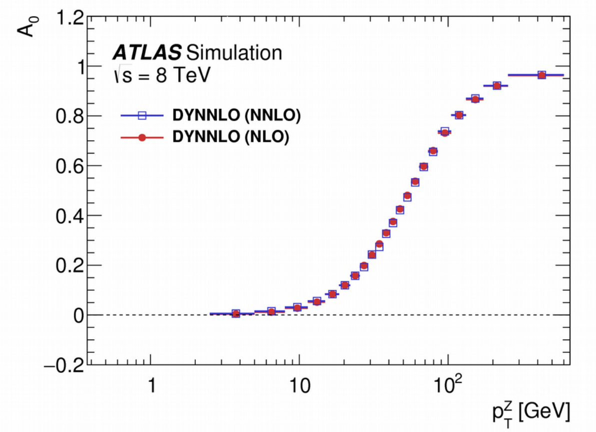

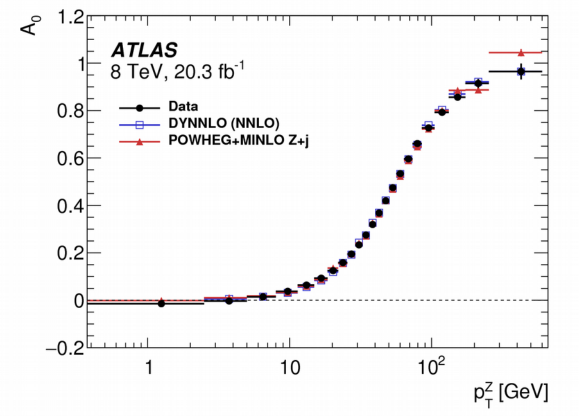

- Also, when including resummation, another intrinsic QCD uncertainty related to the choice of the quantisation axis in the resummed cross section is introduced, which can be addressed f.i with the qt-recoil prescription of DyRes

  Given the very good agreement of data and fixed order NNLO prediction even at very low p_T, is the above uncertainty only a feature of resummed prediction, or does it also affect fixed order calculations?

- Resbos predictions are in poor agreement with fixed order NLO, which is generally close to NNLO, and in perfect agreement with data.

  Is this a feature of Resbos or should we conclude that resummed predictions of the angular coefficients are less accurate then fixed order?

Physics modelling – Summary of QCD uncertainties

W-boson charge	W^+		W^-		Combined	
Kinematic distribution	p_T^ℓ	m_T	p_T^ℓ	m_T	p_T^ℓ	m_T
δm_W [MeV]						
Fixed-order PDF uncertainty	13.1	14.9	12.0	14.2	8.0	8.7
AZ tune	3.0	3.4	3.0	3.4	3.0	3.4
Charm-quark mass	1.2	1.5	1.2	1.5	1.2	1.5
Parton shower μ_F with heavy-flavour decorrelation	5.0	6.9	5.0	6.9	5.0	6.9
Parton shower PDF uncertainty	3.6	4.0	2.6	2.4	1.0	1.6
Angular coefficients	5.8	5.3	5.8	5.3	5.8	5.3
Total	15.9	18.1	14.8	17.2	11.6	12.9

- PDFs are the dominant uncertainty, followed by p_T W uncertainty due to heavy-flavour-initiated production
- PDF uncertainties are partially anti-correlated between W+ and W-, and significantly reduced by the combination of these two categories.
- p_T W uncertainties are similar for m_W extracted from p_T lepton and from m_T

Compatibility of categories

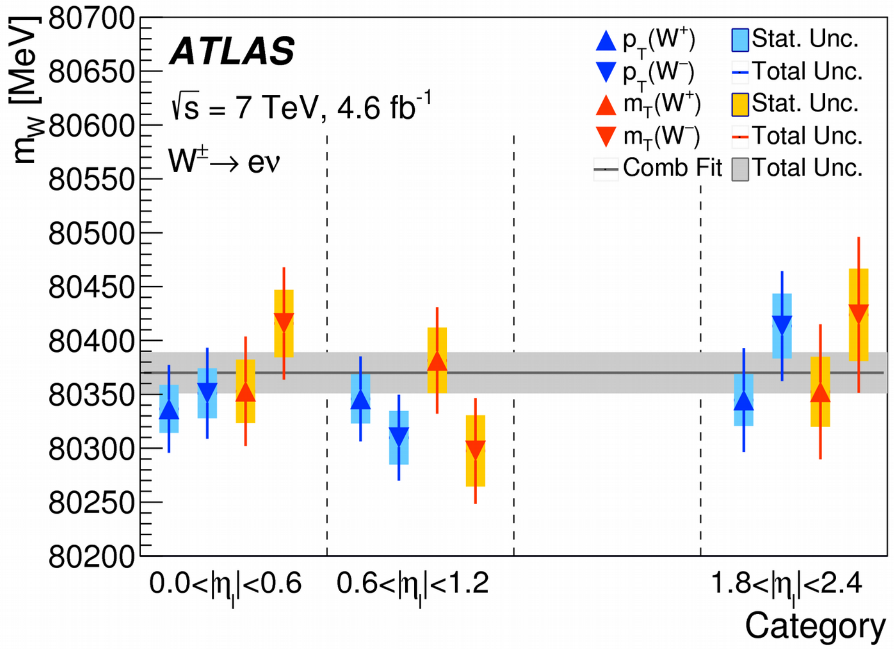

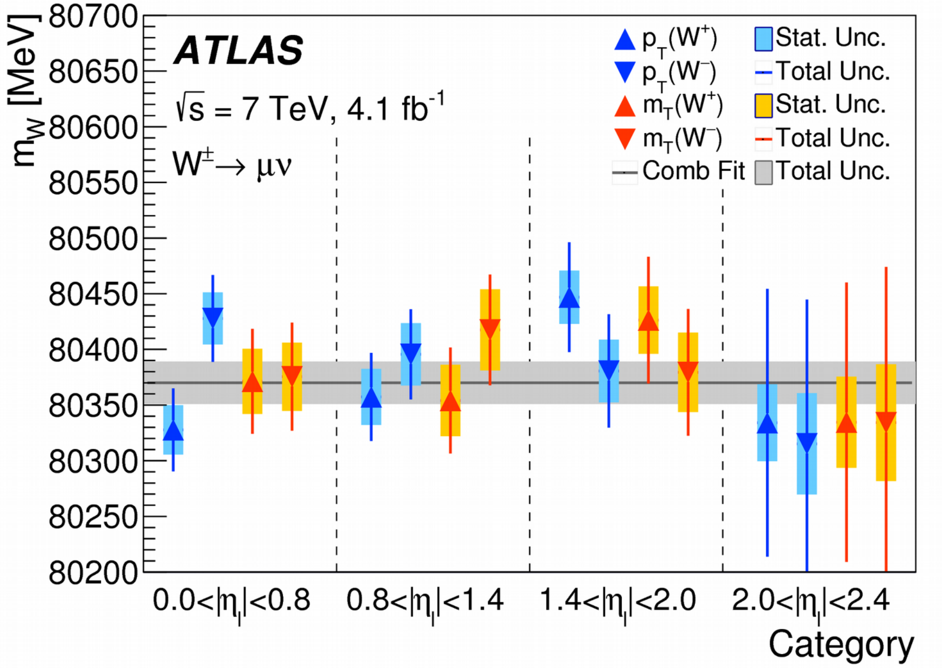

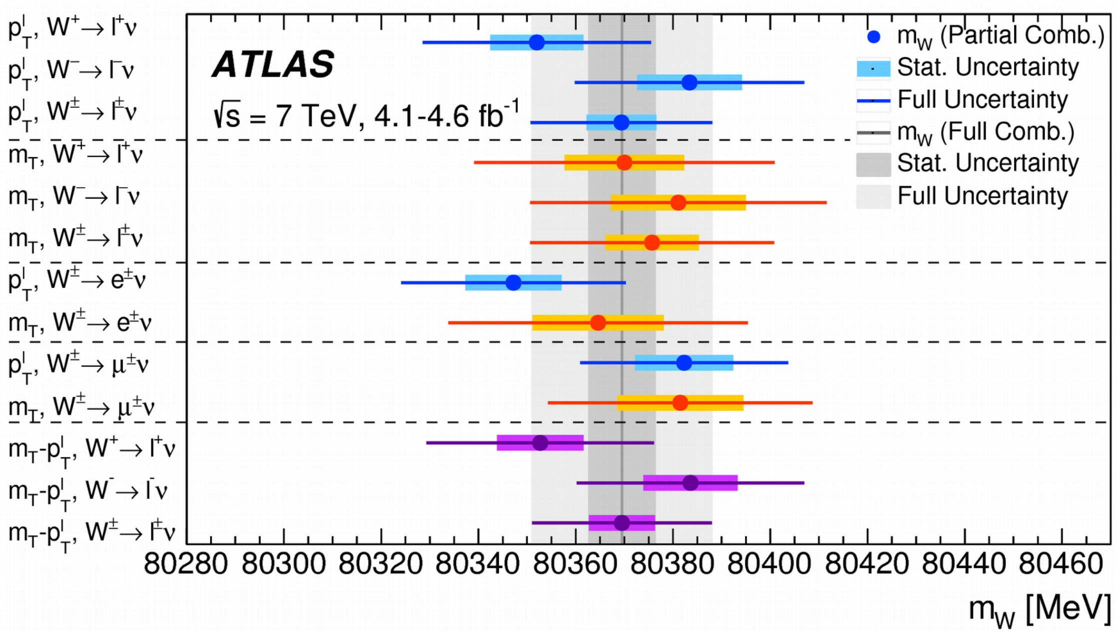

- All categories give consistent extractions of m_W

- Strong validation of physics modelling and detector calibration

Prospects for the physics modelling

- PDF uncertainties can be reduced by the inclusion of precise W, Z inclusive rapidity measurement, currently used only for the validation. Requires work from theorists to include PS corrections in PDF fits.
- p_T W uncertainties can be reduced by using higher-order predictions based on analytical resummation, and with fits to Z pT 8 TeV measurement, which is more precise than the 7 TeV measurement, and has low- and high-mass distributions which can constrain heavy-flavour-initiated production. Usage of higher order predictions requires theorists to understand the discrepancy between PS models and NNLL resummation in the W/Z pt ratio.
- Thanks to the precise measurement at 8 TeV, uncertainties on the angular coefficients are currently not a limiting factor. In the future they can be reduced with more precise measurements and more precise predictions (NNLO V+jet). However, in order to assess the uncertainties with theoretical predictions we still miss a clear prescription.

BACKUP

Summary

- The physics modelling for the measurement of the W mass in ATLAS is built as a composite model which includes EW and QCD corrections
- A fundamental aspect of the model is the use of ancillary DY measurement for validation, and, when possible, to fit the free parameters of the model
- Further validation is provided by Z-boson mass fits, W-boson control plots, and categorisation of the m_W measurement
- Important innovations of the physics modelling with respect to the previous model used at the Tevatron are the treatment of uncertainties of the heavy-flavour-initiated processes, and the NNLO QCD corrections for the angular coefficients and their associated uncertainties

QCD corrections – Drell-Yan decomposition

- At QED born level, and upon integration of additional QCD radiation, the fully differential DY cross sections is a function of 6 lepton variables: px , py , pz , qx , qy , qz
- The DY cross section can be reorganised by factorising the dynamic of the boson production, and the kinematic of the boson decay

$$\frac{d\sigma}{dpdq} = \frac{d^3\sigma}{dp_T dy dm} \sum_i A_i(y, p_T, m) P_i(\cos\theta, \phi)$$

- P_i (cos θ, φ) are spherical harmonics, which provide an orthonormal basis for the decomposition. In the assumption of spin 1 of the boson and spin ½ of the fermions, the 9 harmonics of order 0, 1, and 2 are sufficient for a complete decomposition
- The decomposition is exact at all orders in QCD and LO EW

Which is the formal accuracy of Pythia 8 p_T W?

- Pythia8 implements the so-called "matrix-element" reweighting of the first emission, which make the p_T distribution accurate at $O(\alpha_s)$ at medium/high p_T

Nucl. Phys. B 349 (1991) 635-654

$$P(\alpha_s, z) = \frac{\alpha_s}{2\pi} C_F \frac{1+z^2}{1-z} + \left(\frac{\alpha_s}{\pi}\right)^2 \frac{A^{(2)}}{1-z}$$

$$\alpha_s^{(\mathrm{MC})} = \alpha_s^{(\overline{\mathrm{MS}})}\left(1 + K\frac{\alpha_s^{(\overline{\mathrm{MS}})}}{2\pi}\right)$$

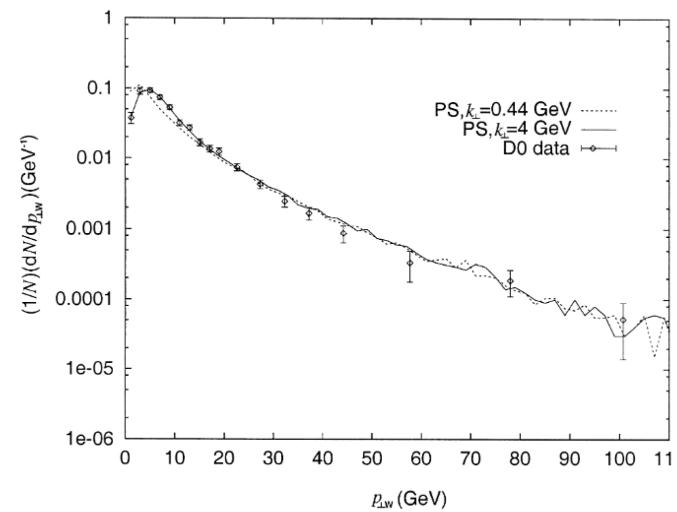

arXiv:hep-ph/9812455

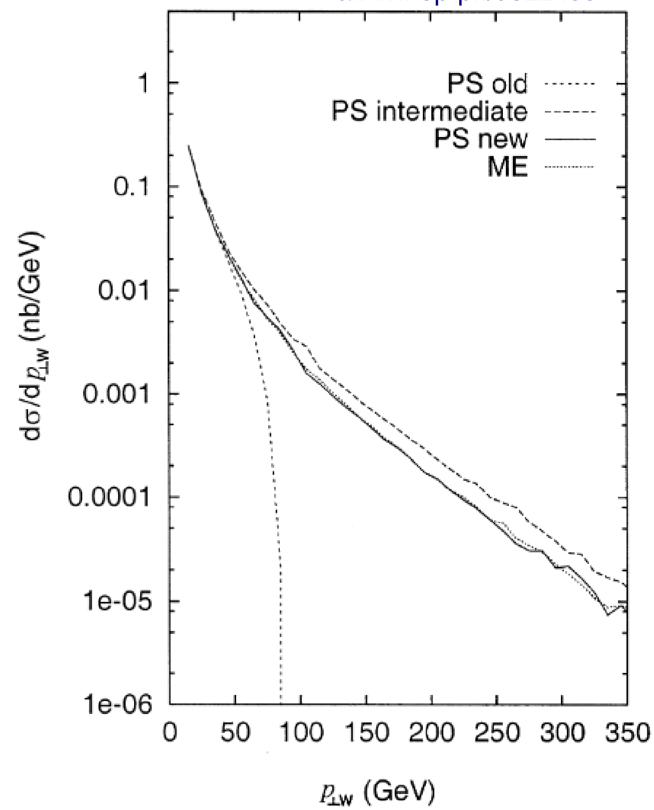

- Resummation arguments show that a set of universal QCD corrections can be absorbed in coherent parton showers by applying the Catani-Marchesini-Webber (CMW) rescaling of the $\overline{\mathrm{MS}}$ value of Λ_{QCD}

$$\alpha_s = 0.118 \rightarrow \alpha_s^{CMW} = 0.126$$

Close to the value α_s= 0.124 of the AZ tune

Is it correct to expect the W p_T normalised distribution of Pythia 8 to be approximately NLO+NLL accurate, i.e. the same formal accuracy of Powheg?

Physics modelling p_T W – Pythia vs Powheg

- We considered also Powheg+Pythia8 and performed a fit to the same p_T Z data, named AZNLO tune
- AZNLO shows similar agreement with data in the inclusive p_T Z distribution, but worse modelling of the rapidity dependent p_T Z distribution

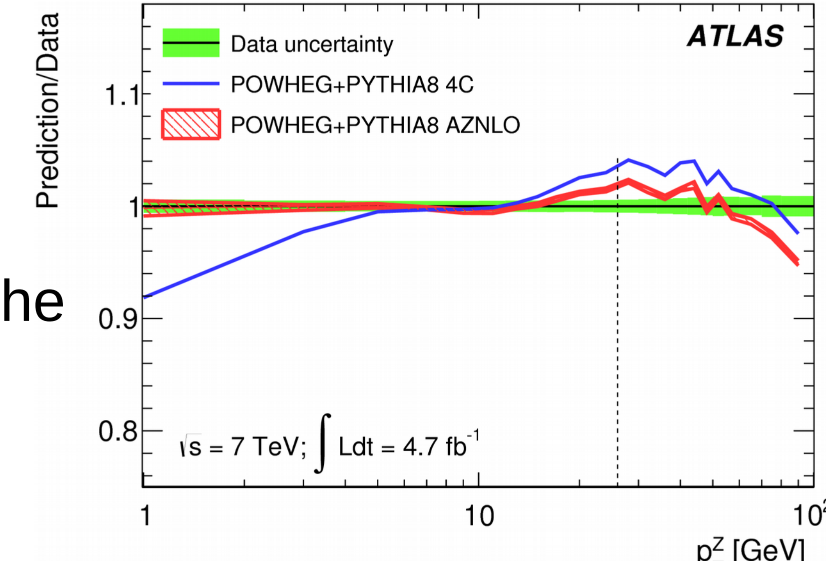

Pythia8 AZ is preferred to Powheg AZNLO

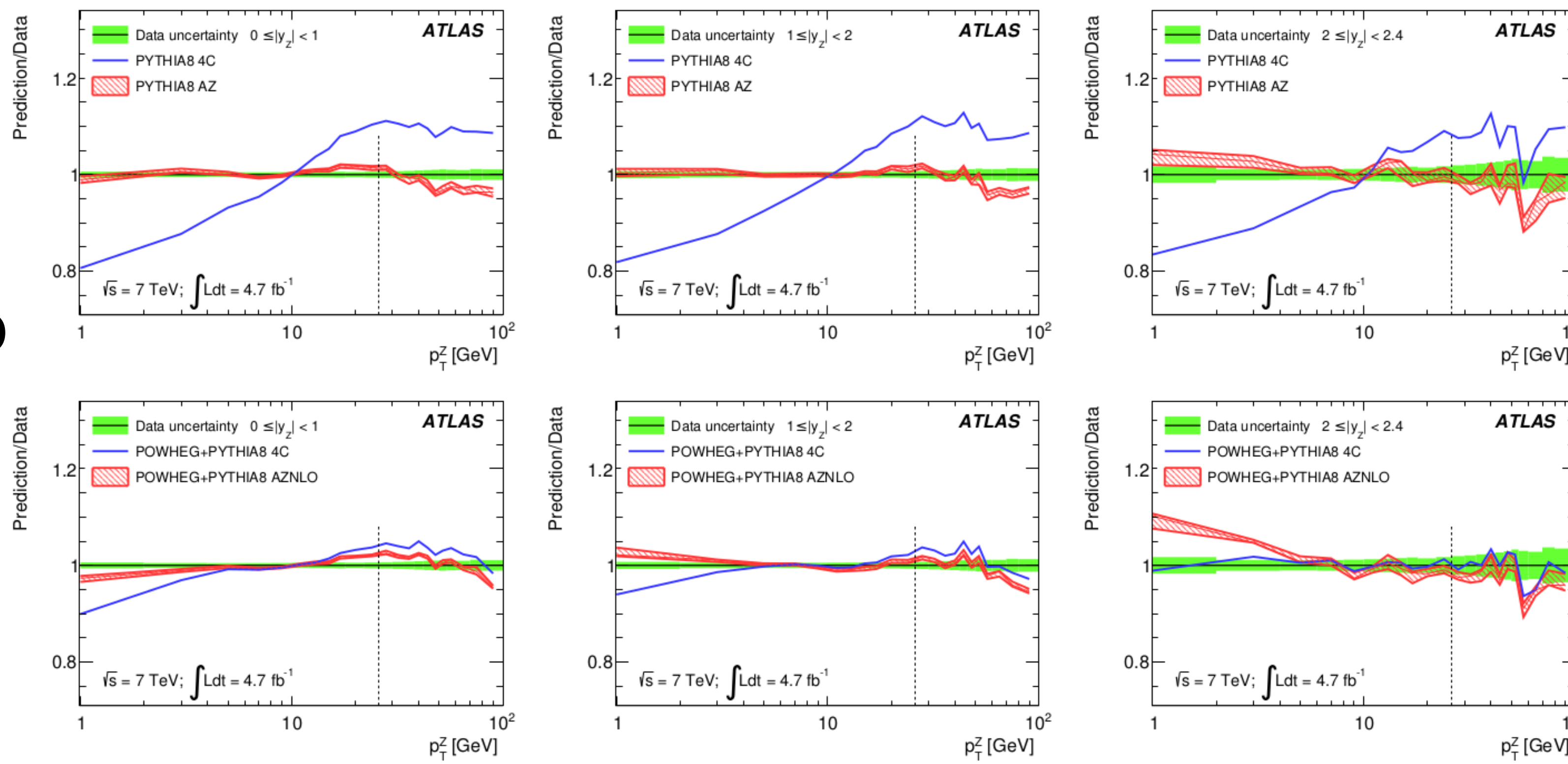

Alternative higher order models for p_T W

- The lack of agreement with data prevented us from using predictions which are formally more accurate (NNLL)
- The effect on the p_T lepton and m_T distributions is large and would shift m_W by O(50-100) MeV

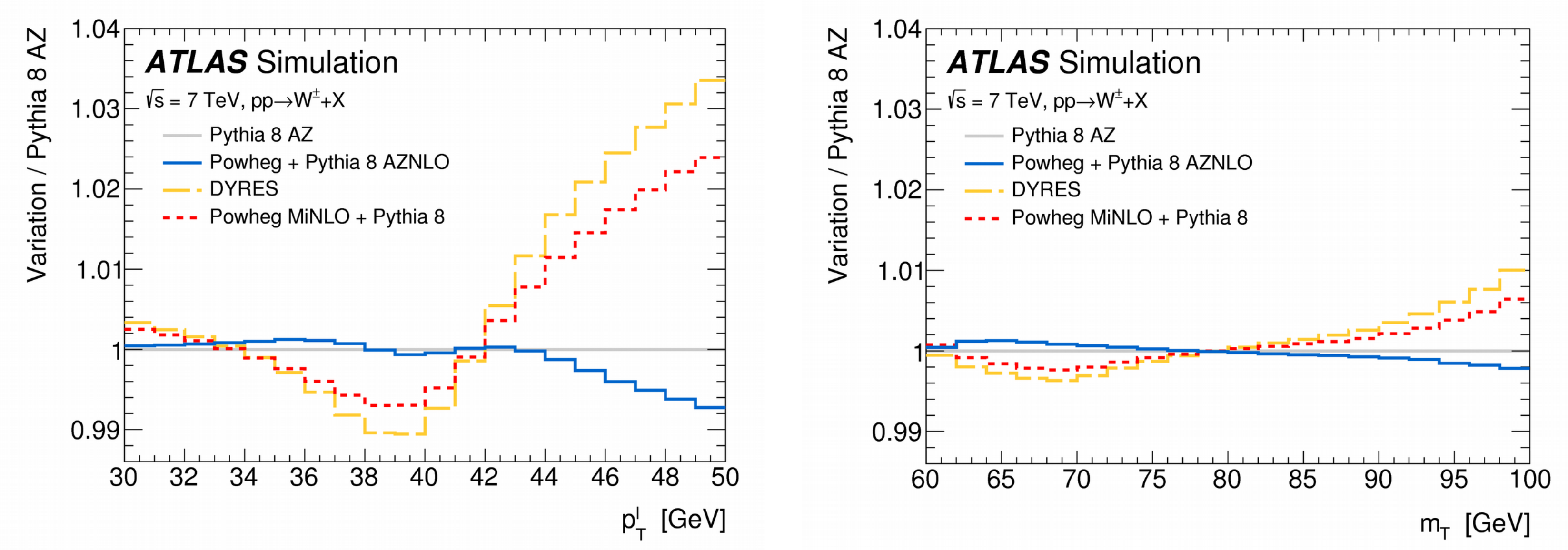

Is this a consequence of

- *Different treatment of heavy-flavour-initiated production?*
- *Corrections to the Sudakov due to multi-parton-interactions?*
- *Poor convergence of the LL, NLL, NNLL series?*
- *What else?*

- FEWZ and DYNNLO agree better than 0.2% for total cross sections, but in the presence of fiducial cuts on the leptons they give significantly different predictions
- FEWZ-DYNNLO: 1.2%(W^+) 0.7%(W^-) 0.2%(Z)
- FEWZ shows a discontinuity of the total cross section as a function of the p_T cut of one of the leptons, when the p_T cuts approach a symmetric configuration, as expected in a fixed order calculation
- DYNNLO is effectively smooth

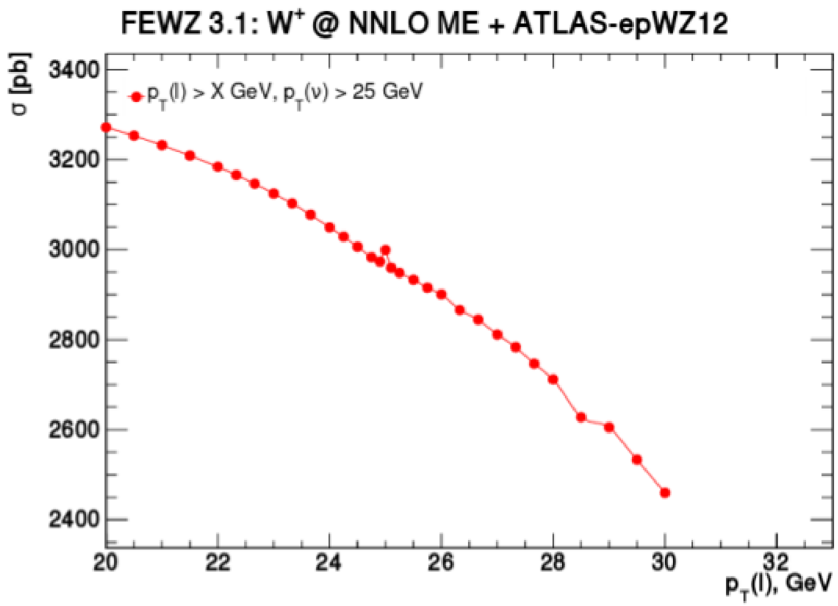

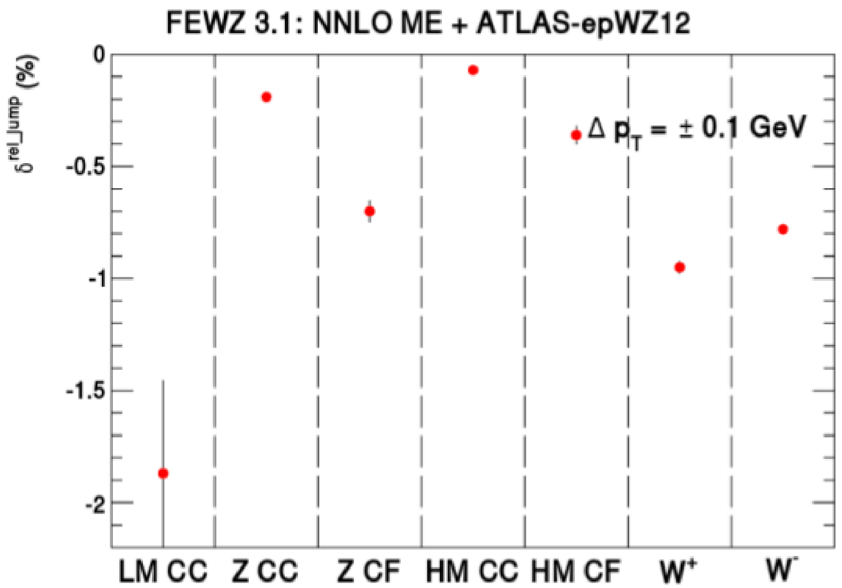

Physics modelling – Rapidity distributions

- FEWZ and DYNNLO differ for the subtraction scheme, sector decomposition in FEWZ and qt-subtraction in DYNNLO
- In DYNNLO, for values of the dilepton p_T below the qtcut (set to $0.008 \cdot m_{ll} \sim$ 0.6-0.7 GeV) the fixed order prediction is approximated by NNLL resummation of logs of p_T/m
- The difference between DYNNLO and FEWZ may be an indication that these large log corrections are significant for fiducial cross sections, and should be accounted for either with parton showers or with analytic resummation

Physics modelling – Rapidity distributions

μ_r	μ_f	χ^2/n.d.f. Total	χ^2/n.d.f. ATLAS	$r_s = \frac{s+\bar{s}}{2\bar{d}}$	$R_s = \frac{s+\bar{s}}{\bar{u}+\bar{d}}$
1	1	1321 / 1102	108 / 61	1.193	1.131
1/2	1/2	1297 / 1102	85 / 61	1.093	1.066
2	2	1329 / 1102	115 / 61	1.270	1.186
1	1/2	1307 / 1102	94 / 61	1.166	1.115
1	2	1312 / 1102	100 / 61	1.201	1.130
1/2	1	1304 / 1102	94 / 61	1.128	1.088
2	1	1321 / 1102	107 / 61	1.241	1.165

- Large variations of the χ^2 associated to variations of the factorisation and renormalisation scales
- Factorisation and renormalisation scales set to $\mu = m_V/2$ are significantly preferred by the data ($\Delta\chi^2 = 23$)

Do we need NNNLO?

Physics modelling – electroweak corrections

- QED FSR: dominant correction, included in the MC with PHOTOS, uncertainty from comparison with YFS. QED ISR also included
- Running widths (and running of α for Z) included in the BW parametrisation
- NLO electroweak: pure weak corrections and ISR-FSR interference, estimated with WINHAC. QCD ISR included to predict a realistic p_T W distribution (at Tevatron it was evaluated at p_T W = 0).
  Estimated and added as uncertainty
- FSR lepton pair production $\gamma^* \rightarrow$ ll : formally higher order (NNLO), but significant correction. Estimated and added as uncertainty

Decay channel	$W \rightarrow e\nu$		$W \rightarrow \mu\nu$	
Kinematic distribution	p_T^ℓ	m_T	p_T^ℓ	m_T
δm_W [MeV]				
FSR (real)	< 0.1	< 0.1	< 0.1	< 0.1
Pure weak and IFI corrections	3.3	2.5	3.5	2.5
FSR (pair production)	3.6	0.8	4.4	0.8
Total	4.9	2.6	5.6	2.6

p_T W uncertainties on p_T lepton and m_T

p_T W uncertainties are similar for m_W extracted from p_T lepton and from m_T

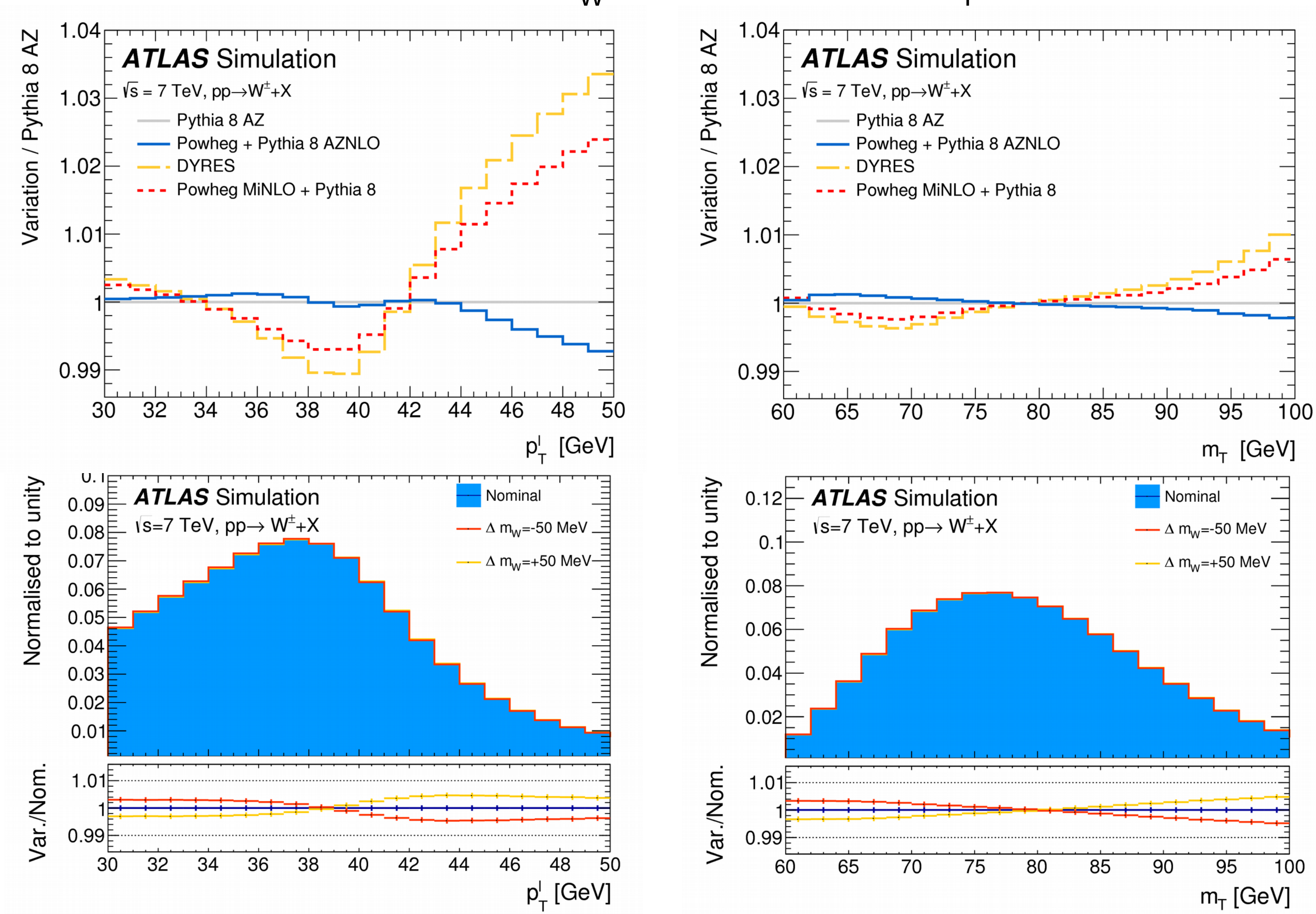

→ m_T is less sensitive to p_T W, but p_T W variations on m_T are less distinguishable from m_W variations

Physics modelling validation – control plots

- The physics modelling (and the detector calibration) is validated with control plots which have little sensitivivity to m_W as u_T, $u_{||}$, $|\eta^l|$

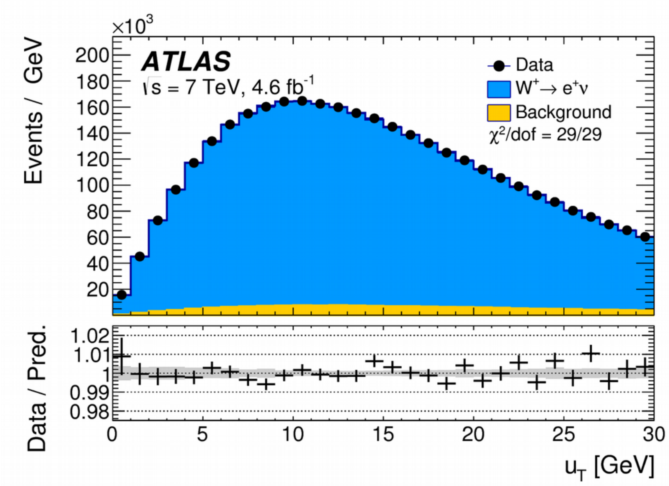

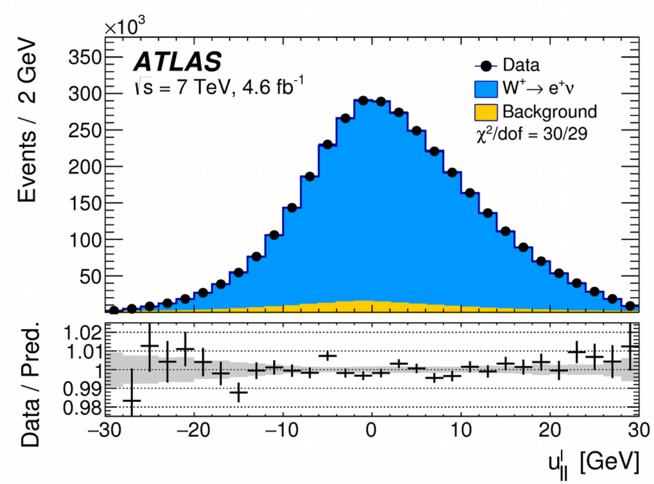

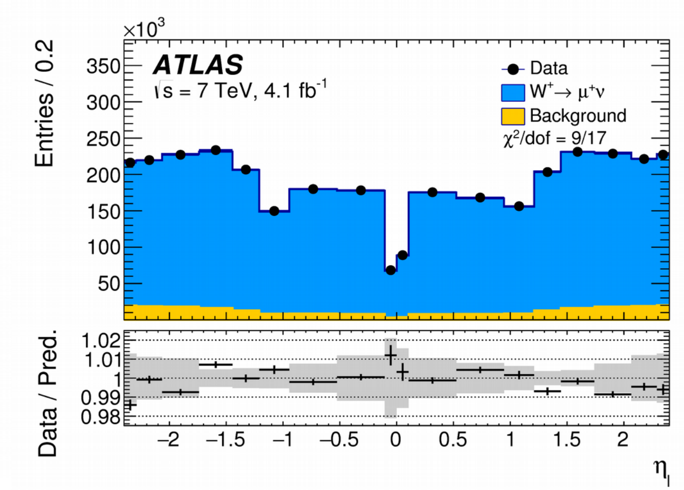

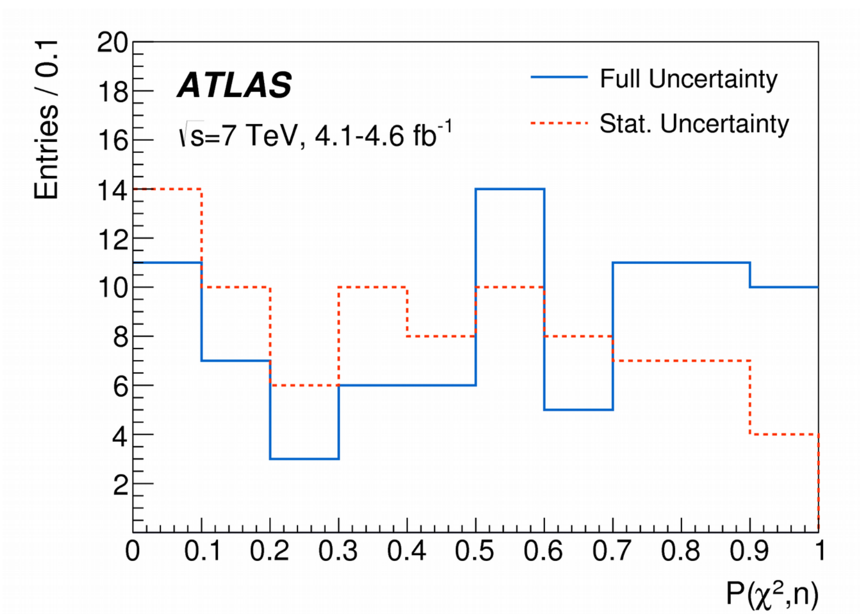

- The distribution of the χ^2 probabilities for the 84 control and post-fit distributions considered in the measurement is flat

Physics modelling validation – categories

- A crucial aspect of the measurement design is the categorisation. The importance of categories is twofold: validate detector calibration and physics modelling and improve accuracy
- The various set of categories are sensitive to different experimental and theoretical biases, the consistency of m_W across categories validates our knowledge of the detector and of QCD
- We considered the measurement ready for unblinding only when all the categories yield consistent values of m_W
- The experimental and theoretical uncertainties have different correlation or anticorrelation patterns, the categorisation allows to constrain them, and increase the sensitivity to m_W
- Categories used for the combination (28 in total):
  p_T lepton – $m_{T,}$ Electrons – muons, $|\eta|$ lepton bins, W+ – W-
- Categories used for cross checks:
  Average $<\mu>$ (pile-up), u_T(recoil), $u_{||}$

LHC vs Tevatron - 1st quark generation

- The m_W measurement in proton-proton collisions is affected by significant complications related to QCD, with respect to proton-antiproton collisions
- W-boson production at the Tevatron is charge symmetric and dominated by interactions with at least one valence quark, whereas the sea-quark PDFs play a larger role at the LHC. The W polarisation at the LHC is more influenced by PDF uncertainties, implying larger uncertainties on the lepton p_T distribution
- The valence-sea difference, as well as the amount of sea quarks with u and d flavour, must be known with better precision than needed at the Tevatron

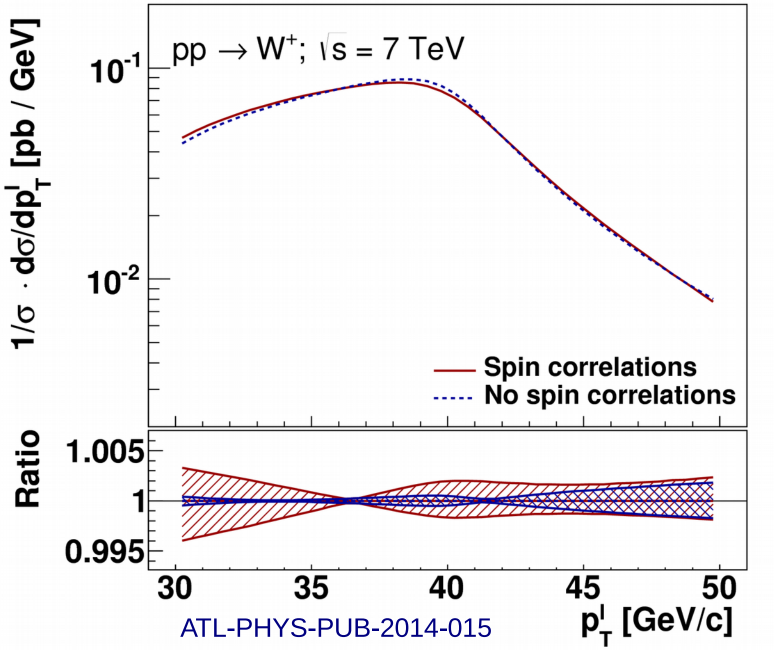

ATL-PHYS-PUB-2014-015

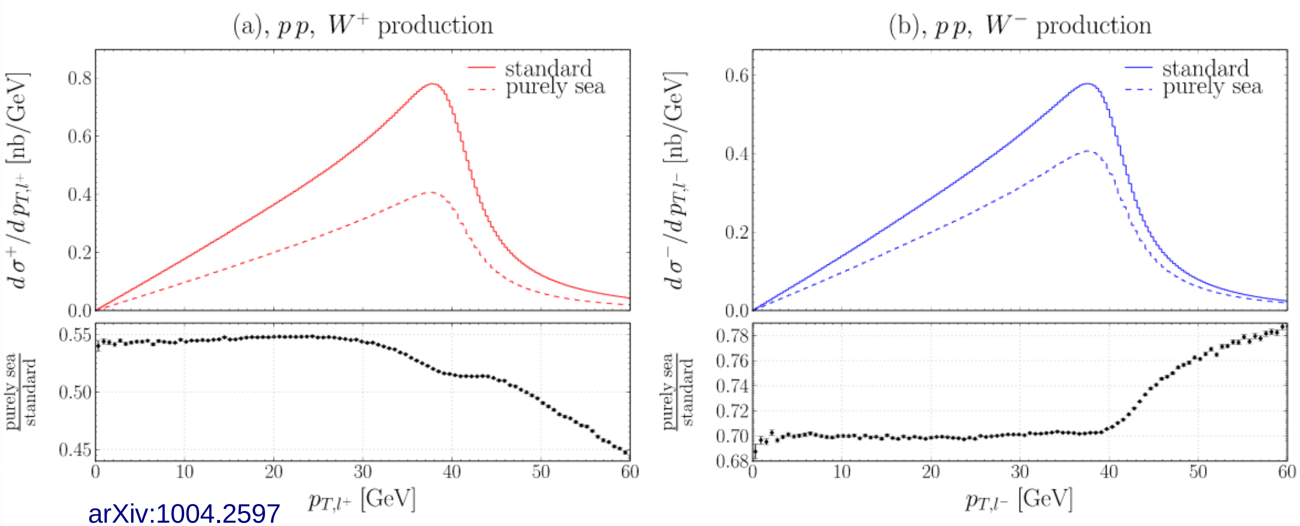

arXiv:1004.2597

LHC vs Tevatron - 2nd quark generation

- At sqrt(s) = 7 TeV, approximately 25% of the W-boson production is induced by at least one second-generation quark, s or c, in the initial state. The amount of heavy-quark-initiated production has implications for the W-boson transverse-momentum distribution and for the W polarisation

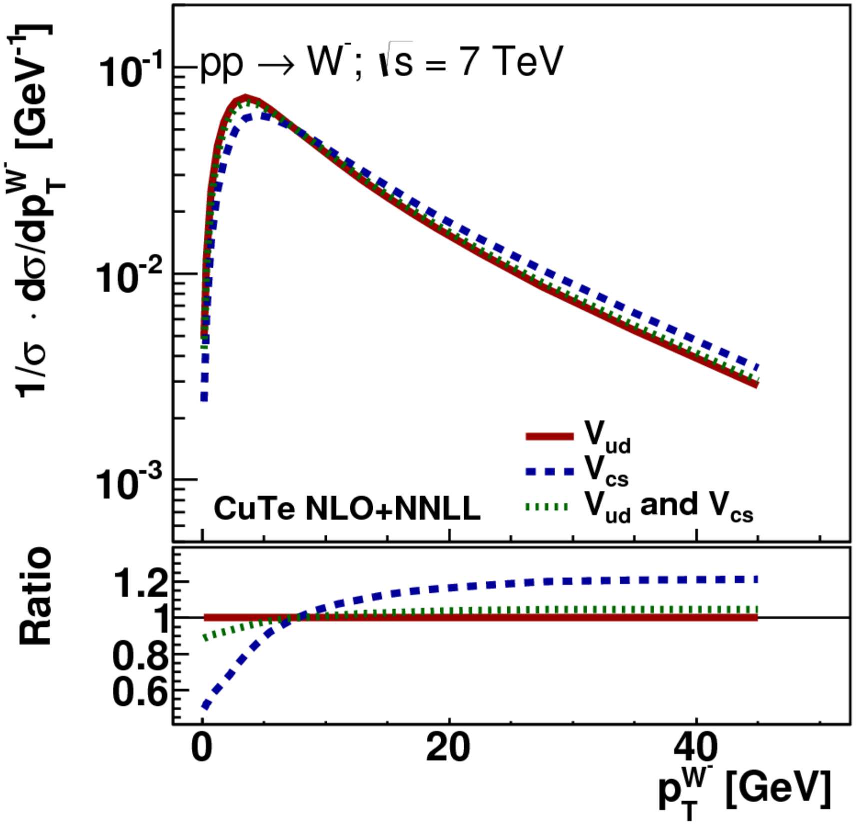

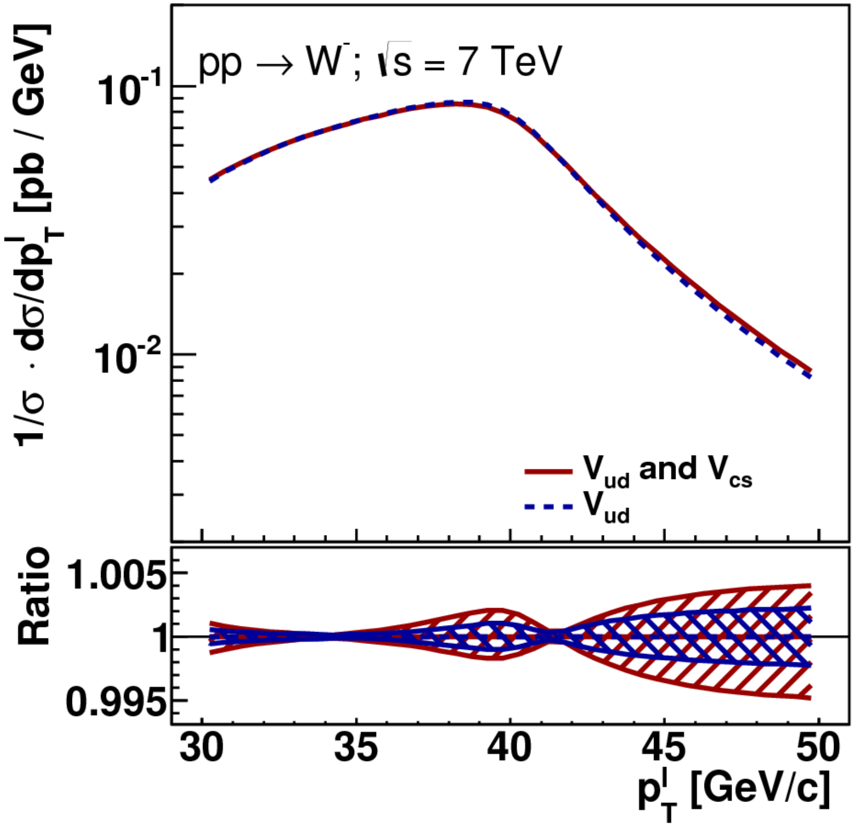

Comparison of uncertainties with CDF

Similar PDF uncertainties

p_T W uncertainties are larger for p_T lepton than m_T at CDF, but similar in ATLAS

m_T fit uncertainties			
Source	$W \to \mu\nu$	$W \to e\nu$	Common
Lepton energy scale	7	10	5
Lepton energy resolution	1	4	0
Lepton efficiency	0	0	0
Lepton tower removal	2	3	2
Recoil scale	5	5	5
Recoil resolution	7	7	7
Backgrounds	3	4	0
PDFs	10	10	10
W boson p_T	3	3	3
Photon radiation	4	4	4
Statistical	16	19	0
Total	23	26	15

p_T^ℓ fit uncertainties			
Source	$W \to \mu\nu$	$W \to e\nu$	Common
Lepton energy scale	7	10	5
Lepton energy resolution	1	4	0
Lepton efficiency	1	2	0
Lepton tower removal	0	0	0
Recoil scale	6	6	6
Recoil resolution	5	5	5
Backgrounds	5	3	0
PDFs	9	9	9
W boson p_T	9	9	9
Photon radiation	4	4	4
Statistical	18	21	0
Total	25	28	16

Includes also Ai uncertainties

Combined categories	Value [MeV]	Stat. Unc.	Muon Unc.	Elec. Unc.	Recoil Unc.	Bckg. Unc.	QCD Unc.	EW Unc.	PDF Unc.	Total Unc.	χ^2/dof of Comb.
$p_T^\ell, W^\pm, e$	80347.2	9.9	0.0	14.8	2.6	5.7	8.2	5.3	8.9	23.1	4/5
$m_T, W^\pm, e$	80364.6	13.5	0.0	14.4	13.2	12.8	9.5	3.4	10.2	30.8	8/5
$p_T^\ell, W^\pm, \mu$	80382.3	10.1	10.7	0.0	2.5	3.9	8.4	6.0	10.7	21.4	7/7
$m_T, W^\pm, \mu$	80381.5	13.0	11.6	0.0	13.0	6.0	9.6	3.4	11.2	27.2	3/7

Comparison of uncertainties with D0

Source	Section	m_T	p_T^e	$\not{E}_T$
Experimental				
Electron Energy Scale	VII C 4	16	17	16
Electron Energy Resolution	VII C 5	2	2	3
Electron Shower Model	V C	4	6	7
Electron Energy Loss	V D	4	4	4
Recoil Model	VII D 3	5	6	14
Electron Efficiencies	VII B 10	1	3	5
Backgrounds	VIII	2	2	2
$\sum$(Experimental)		18	20	24
W Production and Decay Model				
PDF	VI C	11	11	14
QED	VI B	7	7	9
Boson p_T	VI A	2	5	2
$\sum$(Model)		13	14	17
Systematic Uncertainty (Experimental and Model)		22	24	29
W Boson Statistics	IX	13	14	15
Total Uncertainty		26	28	33

Similar PDF uncertainties

Smaller p_T W uncertainties at D0

Includes also Ai uncertainties

Combined categories	Value [MeV]	Stat. Unc.	Muon Unc.	Elec. Unc.	Recoil Unc.	Bckg. Unc.	QCD Unc.	EW Unc.	PDF Unc.	Total Unc.	χ^2/dof of Comb.
p_T^ℓ, $W^\pm$, e	80347.2	9.9	0.0	14.8	2.6	5.7	8.2	5.3	8.9	23.1	4/5
m_T, $W^\pm$, e	80364.6	13.5	0.0	14.4	13.2	12.8	9.5	3.4	10.2	30.8	8/5
p_T^ℓ, $W^\pm$, μ	80382.3	10.1	10.7	0.0	2.5	3.9	8.4	6.0	10.7	21.4	7/7
m_T, $W^\pm$, μ	80381.5	13.0	11.6	0.0	13.0	6.0	9.6	3.4	11.2	27.2	3/7

Physics modelling – electroweak corrections

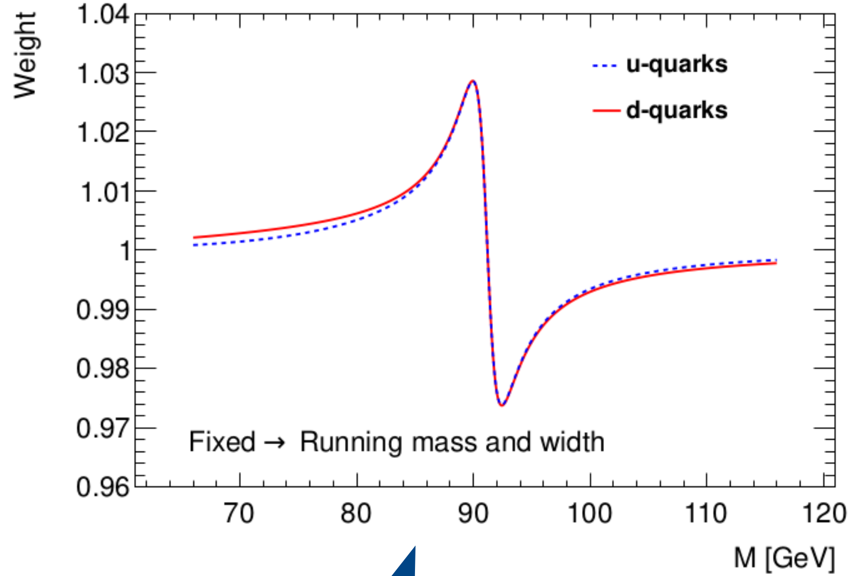

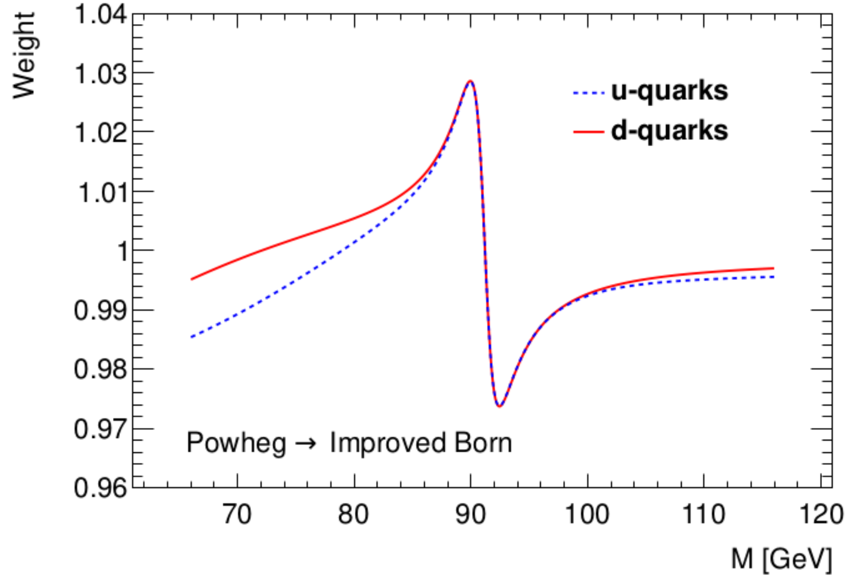

Running width

$$P'_{ij}(\hat{s}) = \hat{s}\,\frac{(\hat{s}-m'^2_i)(\hat{s}-m'^2_j)+\frac{\hat{s}^2}{m'_i m'_j}\Gamma'_i\Gamma'_j}{\left[(\hat{s}-m'^2_i)^2+(\frac{\hat{s}}{m'_i}\Gamma'_i)^2\right]\left[(\hat{s}-m'^2_j)^2+(\frac{\hat{s}}{m'_j}\Gamma'_j)^2\right]}$$

$$\alpha_{\text{em}}(s) = \frac{\alpha_{\text{em}}(0)}{1-\Delta\alpha(s)};$$

$$\Delta\alpha(s) = \frac{\alpha_{\text{em}}(0)}{3\pi}(13.4955+3\ln s)+0.00165+0.00299\ln(1+s).$$

Running α

Physics modelling – electroweak corrections

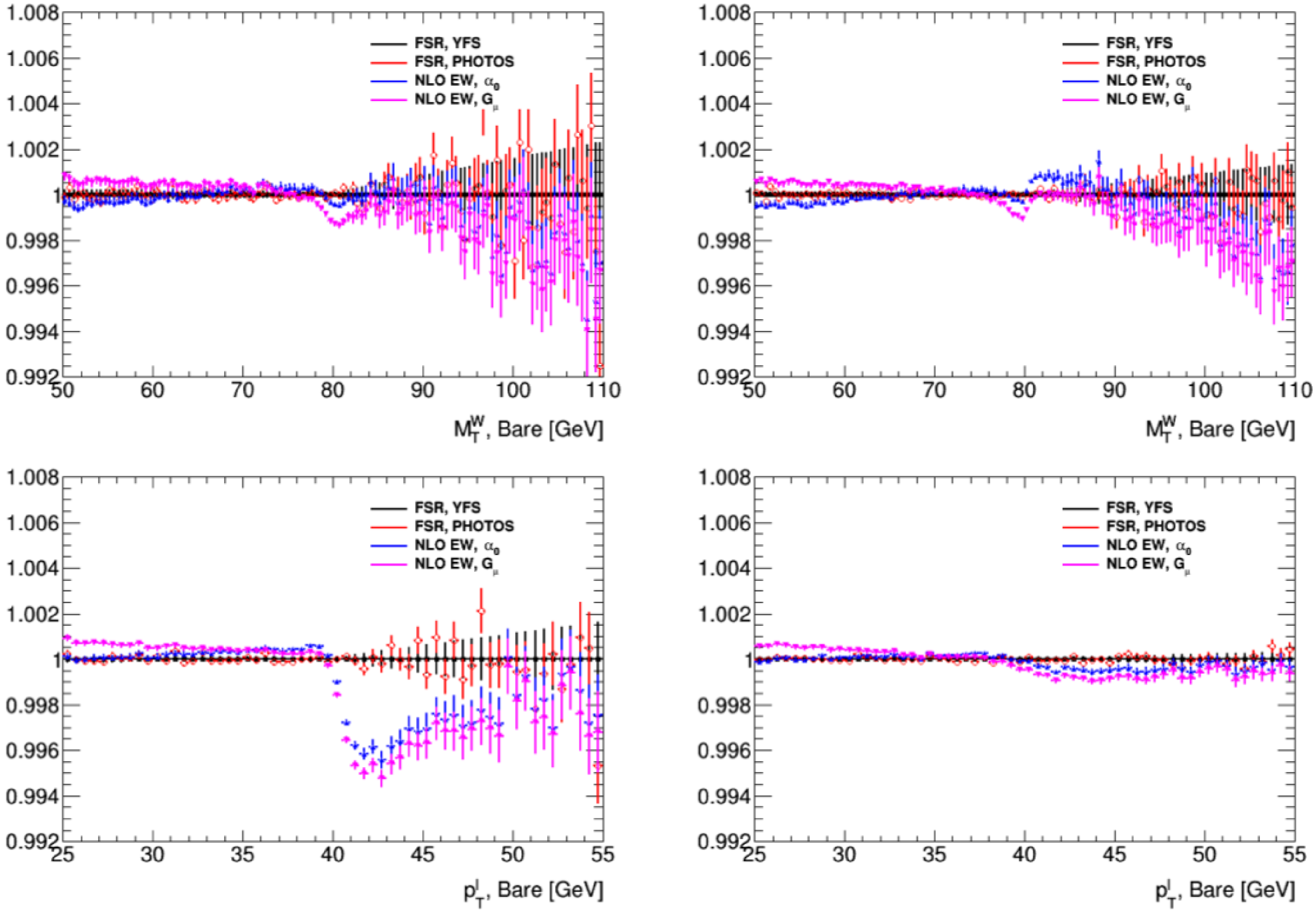

Physics modelling validation – Z-boson mass

- The physics modelling (and the detector calibration) is first validated by performing an extraction of m_Z
- The extraction is a closure test, and not a measurement of m_Z, because the LEP measurement is used as input for detector calibration

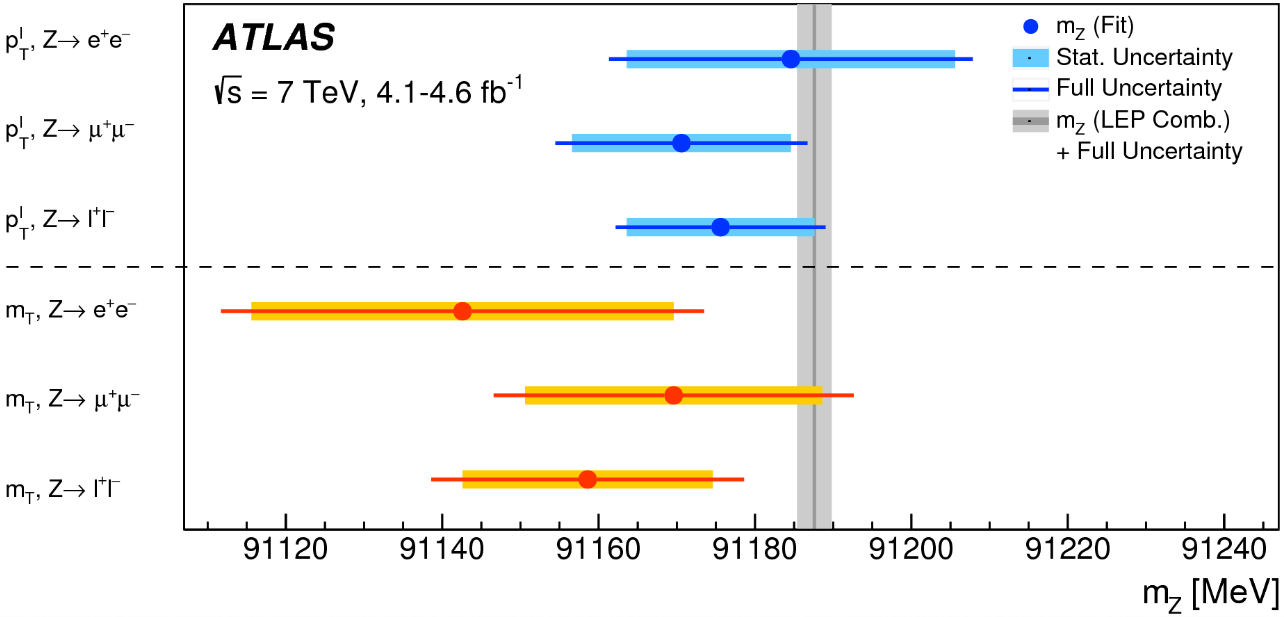

Lepton charge	ℓ^+		ℓ^-		Combined	
Distribution	p_T^ℓ	m_T	p_T^ℓ	m_T	p_T^ℓ	m_T
Δm_Z [MeV]						
$Z \to ee$	$13 \pm 31 \pm 10$	$-93 \pm 38 \pm 15$	$-20 \pm 31 \pm 10$	$4 \pm 38 \pm 15$	$-3 \pm 21 \pm 10$	$-45 \pm 27 \pm 15$
$Z \to \mu\mu$	$1 \pm 22 \pm 8$	$-35 \pm 28 \pm 13$	$-36 \pm 22 \pm 8$	$-1 \pm 27 \pm 13$	$-17 \pm 14 \pm 8$	$-18 \pm 19 \pm 13$
Combined	$5 \pm 18 \pm 6$	$-58 \pm 23 \pm 12$	$-31 \pm 18 \pm 6$	$1 \pm 22 \pm 12$	$-12 \pm 12 \pm 6$	$-29 \pm 16 \pm 12$

Z-boson angular coefficients at 8 TeV

- A cos(2ϕ) asymmetry which violates the Lam-Tung relation at low pt was observed in fixed target experiments

$$P_2(\cos\theta,\phi) = \frac{1}{2}\sin^2\theta\cos 2\phi \qquad \frac{d\sigma}{d\Omega} \propto 1 + \lambda\cos^2\theta + \mu\sin 2\theta\cos\phi + \frac{\nu}{2}\sin^2\theta\cos 2\phi$$

➡ ν = A2

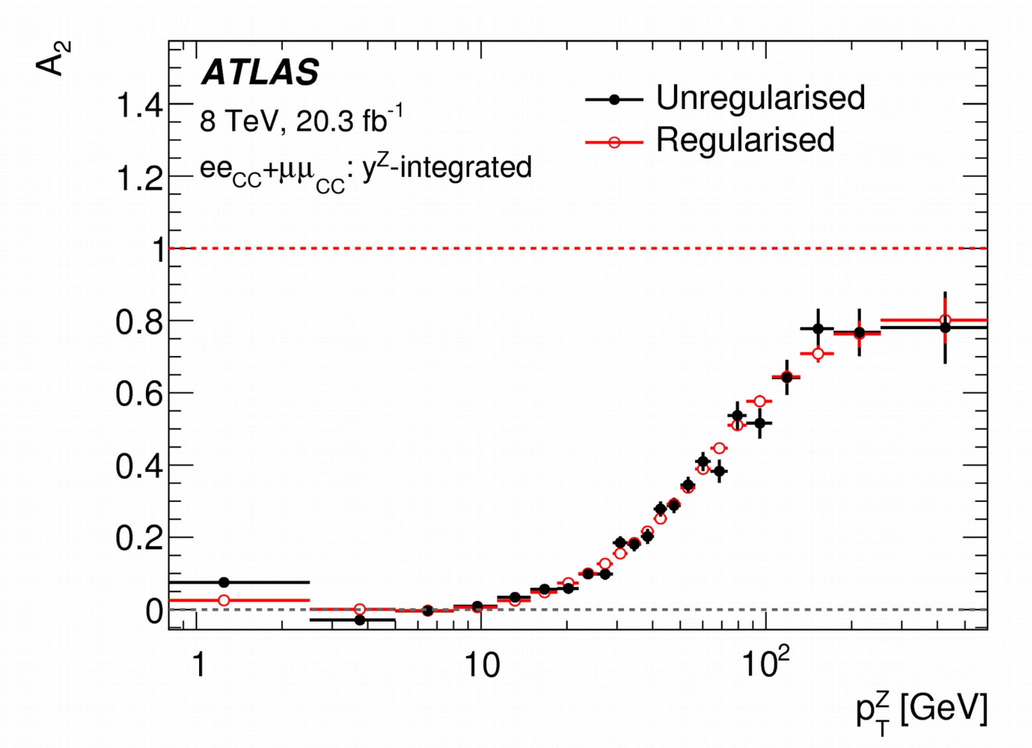

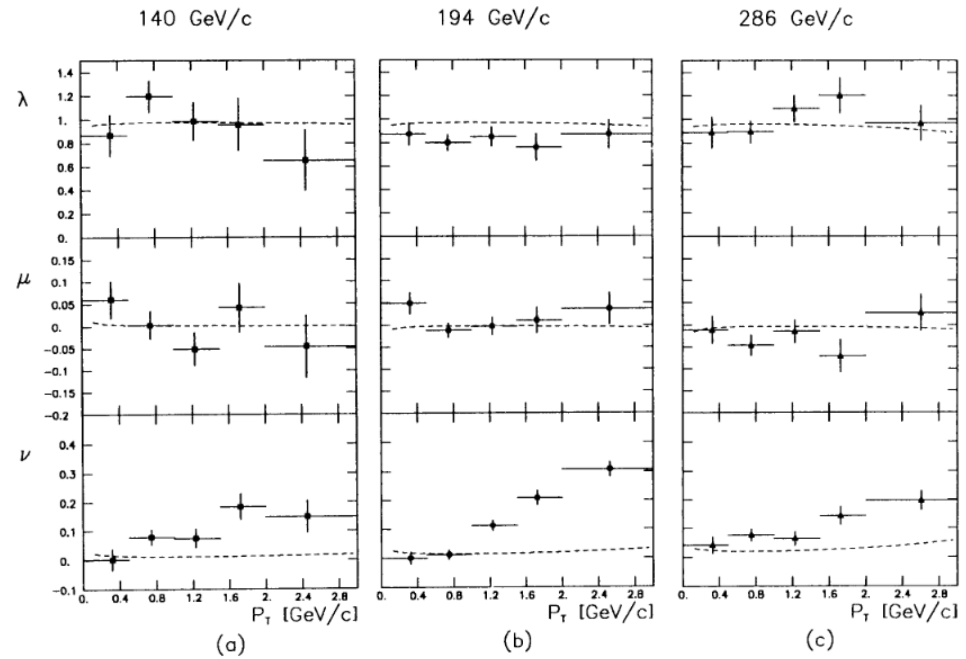

Fig. 3a–c. Parameters λ, μ, and ν as a function of P_T in the CS frame. **a** 140 GeV/c; **b** 194 GeV/c; **c** 286 GeV/c. The error bars correspond to the statistical uncertainties only. The horizontal bars give the size of each interval. The dashed curves are the predictions of perturbative QCD [3]

A2 at low p_T

- A cos(2ϕ) asymmetry which violates the Lam-Tung relation at low pt was observed in fixed target experiments
- The effect can be explained by higher twist effects, QCD vacuum effects, or by the Boer-Mulders TMD functions, which describe a correlation between transverse momentum and transverse spin of quarks

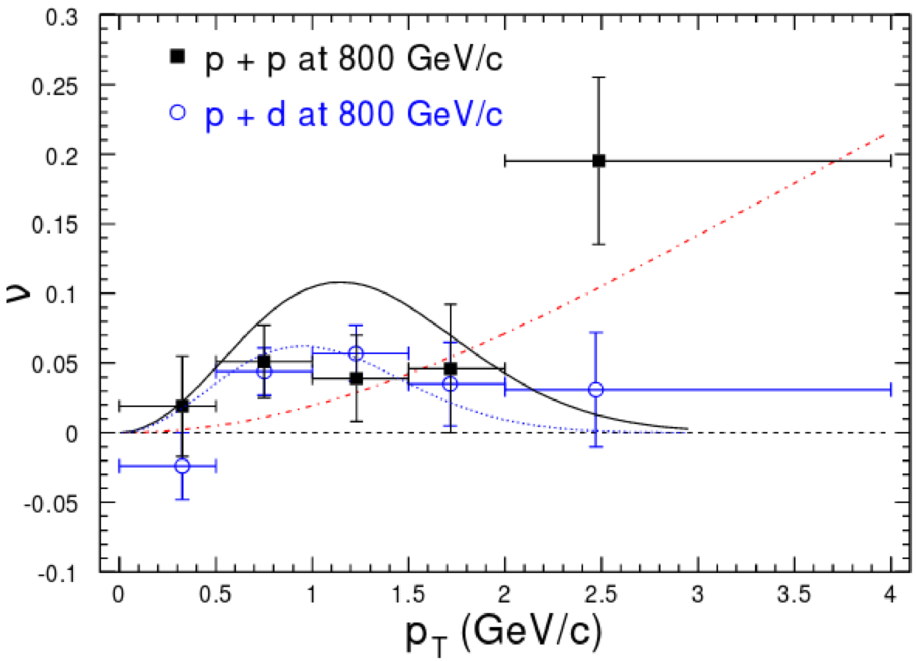

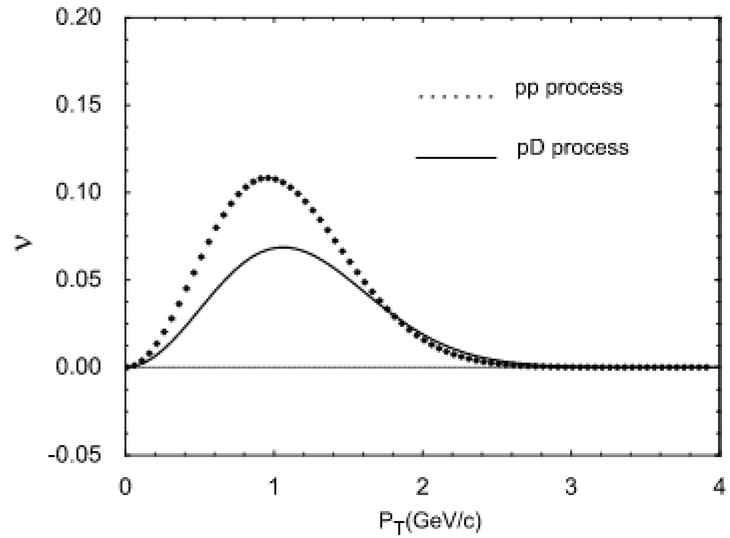

FIG. 4: The p_T-dependent $\cos 2\phi$ asymmetries ν in both pp (dotted curve)and pD(solid curve) Drell-Yan processes at FNAL E866/NuSea, calculated with the fitted Boer-Mulders functions presented in Table I.

What is the possible influence on the W mass measurement

Control plots - electrons

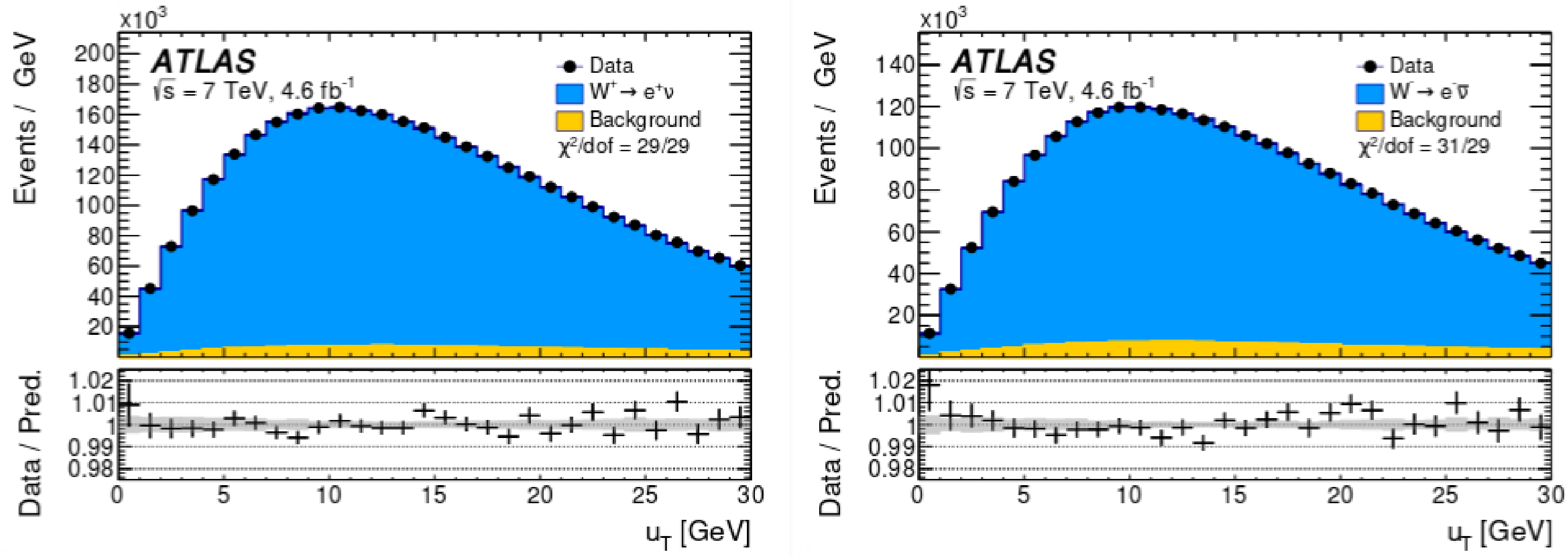

(c) (d)

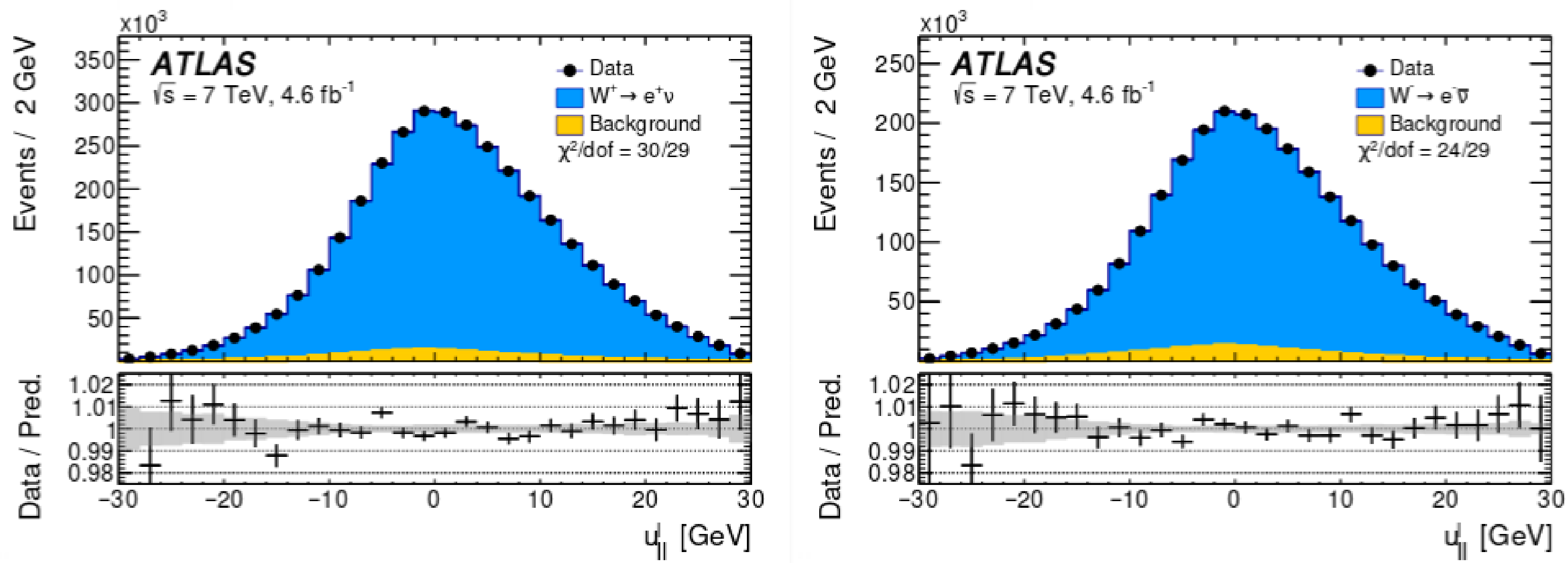

Control plots - muons

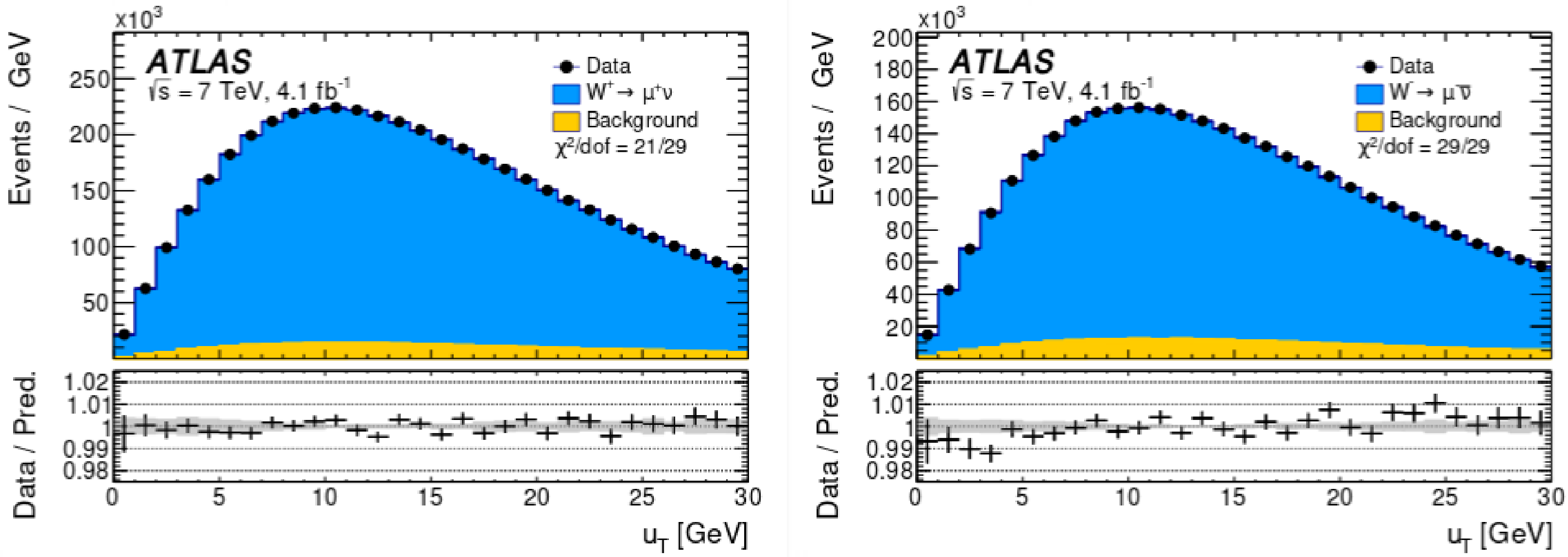

(c) (d)

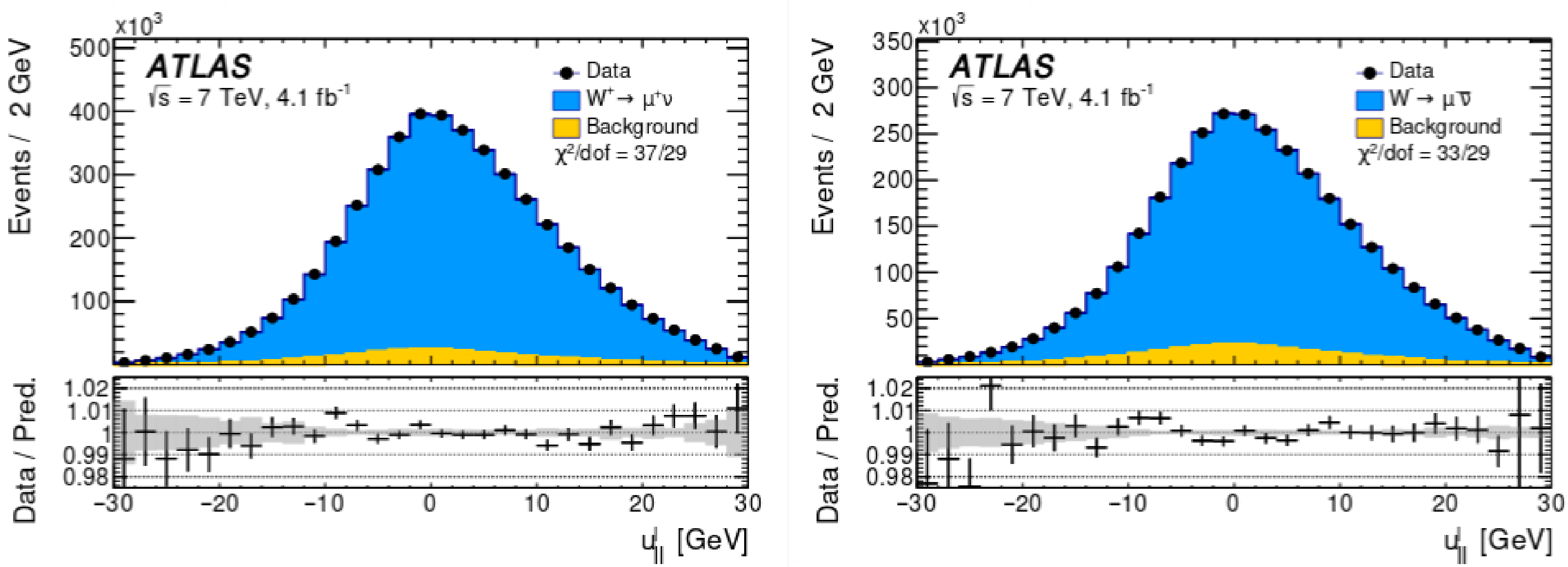

Measurement categories

Channel m_T-Fit	m_W [MeV]	Stat. Unc.	Muon Unc.	Elec. Unc.	Recoil Unc.	Bckg. Unc.	QCD Unc.	EW Unc.	PDF Unc.	Total Unc.
$W^+ \to \mu\nu, \lvert\eta\rvert < 0.8$	80371.3	29.2	12.4	0.0	15.2	8.1	9.9	3.4	28.4	47.1
$W^+ \to \mu\nu, 0.8 < \lvert\eta\rvert < 1.4$	80354.1	32.1	19.3	0.0	13.0	6.8	9.6	3.4	23.3	47.6
$W^+ \to \mu\nu, 1.4 < \lvert\eta\rvert < 2.0$	80426.3	30.2	35.1	0.0	14.3	7.2	9.3	3.4	27.2	56.9
$W^+ \to \mu\nu, 2.0 < \lvert\eta\rvert < 2.4$	80334.6	40.9	112.4	0.0	14.4	9.0	8.4	3.4	32.8	125.5
$W^- \to \mu\nu, \lvert\eta\rvert < 0.8$	80375.5	30.6	11.6	0.0	13.1	8.5	9.5	3.4	30.6	48.5
$W^- \to \mu\nu, 0.8 < \lvert\eta\rvert < 1.4$	80417.5	36.4	18.5	0.0	12.2	7.7	9.7	3.4	22.2	49.7
$W^- \to \mu\nu, 1.4 < \lvert\eta\rvert < 2.0$	80379.4	35.6	33.9	0.0	10.5	8.1	9.7	3.4	23.1	56.9
$W^- \to \mu\nu, 2.0 < \lvert\eta\rvert < 2.4$	80334.2	52.4	123.7	0.0	11.6	10.2	9.9	3.4	34.1	139.9
$W^+ \to e\nu, \lvert\eta\rvert < 0.6$	80352.9	29.4	0.0	19.5	13.1	15.3	9.9	3.4	28.5	50.8
$W^+ \to e\nu, 0.6 < \lvert\eta\rvert < 1.2$	80381.5	30.4	0.0	21.4	15.1	13.2	9.6	3.4	23.5	49.4
$W^+ \to e\nu, 1,8 < \lvert\eta\rvert < 2.4$	80352.4	32.4	0.0	26.6	16.4	32.8	8.4	3.4	27.3	62.6
$W^- \to e\nu, \lvert\eta\rvert < 0.6$	80415.8	31.3	0.0	16.4	11.8	15.5	9.5	3.4	31.3	52.1
$W^- \to e\nu, 0.6 < \lvert\eta\rvert < 1.2$	80297.5	33.0	0.0	18.7	11.2	12.8	9.7	3.4	23.9	49.0
$W^- \to e\nu, 1.8 < \lvert\eta\rvert < 2.4$	80423.8	42.8	0.0	33.2	12.8	35.1	9.9	3.4	28.1	72.3
p_T-Fit										
$W^+ \to \mu\nu, \lvert\eta\rvert < 0.8$	80327.7	22.1	12.2	0.0	2.6	5.1	9.0	6.0	24.7	37.3
$W^+ \to \mu\nu, 0.8 < \lvert\eta\rvert < 1.4$	80357.3	25.1	19.1	0.0	2.5	4.7	8.9	6.0	20.6	39.5
$W^+ \to \mu\nu, 1.4 < \lvert\eta\rvert < 2.0$	80446.9	23.9	33.1	0.0	2.5	4.9	8.2	6.0	25.2	49.3
$W^+ \to \mu\nu, 2.0 < \lvert\eta\rvert < 2.4$	80334.1	34.5	110.1	0.0	2.5	6.4	6.7	6.0	31.8	120.2
$W^- \to \mu\nu, \lvert\eta\rvert < 0.8$	80427.8	23.3	11.6	0.0	2.6	5.8	8.1	6.0	26.4	39.0
$W^- \to \mu\nu, 0.8 < \lvert\eta\rvert < 1.4$	80395.6	27.9	18.3	0.0	2.5	5.6	8.0	6.0	19.8	40.5
$W^- \to \mu\nu, 1.4 < \lvert\eta\rvert < 2.0$	80380.6	28.1	35.2	0.0	2.6	5.6	8.0	6.0	20.6	50.9
$W^- \to \mu\nu, 2.0 < \lvert\eta\rvert < 2.4$	80315.2	45.5	116.1	0.0	2.6	7.6	8.3	6.0	32.7	129.6
$W^+ \to e\nu, \lvert\eta\rvert < 0.6$	80336.5	22.2	0.0	20.1	2.5	6.4	9.0	5.3	24.5	40.7
$W^+ \to e\nu, 0.6 < \lvert\eta\rvert < 1.2$	80345.8	22.8	0.0	21.4	2.6	6.7	8.9	5.3	20.5	39.4
$W^+ \to e\nu, 1,8 < \lvert\eta\rvert < 2.4$	80344.7	24.0	0.0	30.8	2.6	11.9	6.7	5.3	24.1	48.2
$W^- \to e\nu, \lvert\eta\rvert < 0.6$	80351.0	23.1	0.0	19.8	2.6	7.2	8.1	5.3	26.6	42.2
$W^- \to e\nu, 0.6 < \lvert\eta\rvert < 1.2$	80309.8	24.9	0.0	19.7	2.7	7.3	8.0	5.3	20.9	39.9
$W^- \to e\nu, 1.8 < \lvert\eta\rvert < 2.4$	80413.4	30.1	0.0	30.7	2.7	11.5	8.3	5.3	22.7	51.0

Post fit plots - electrons

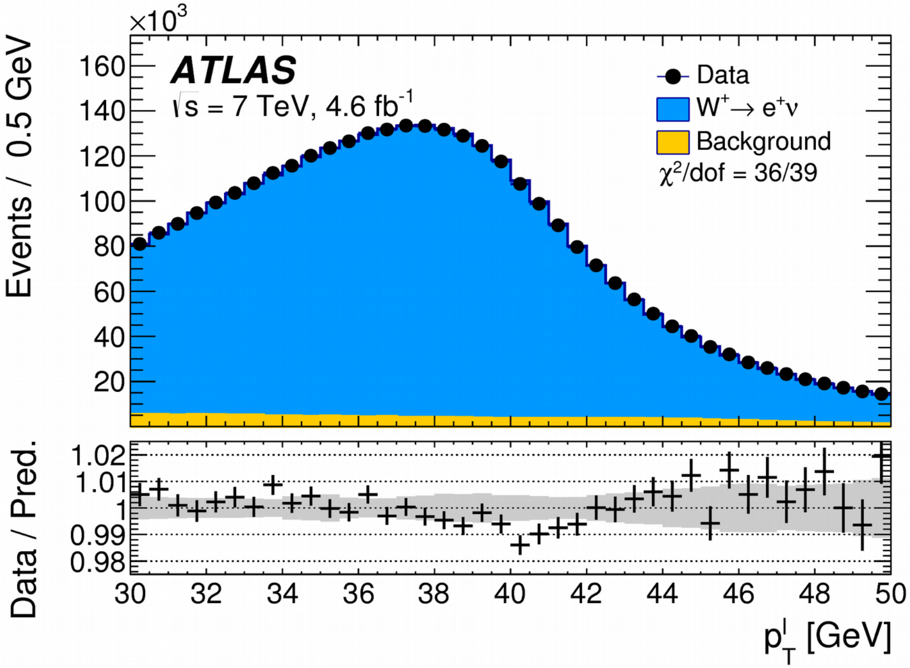

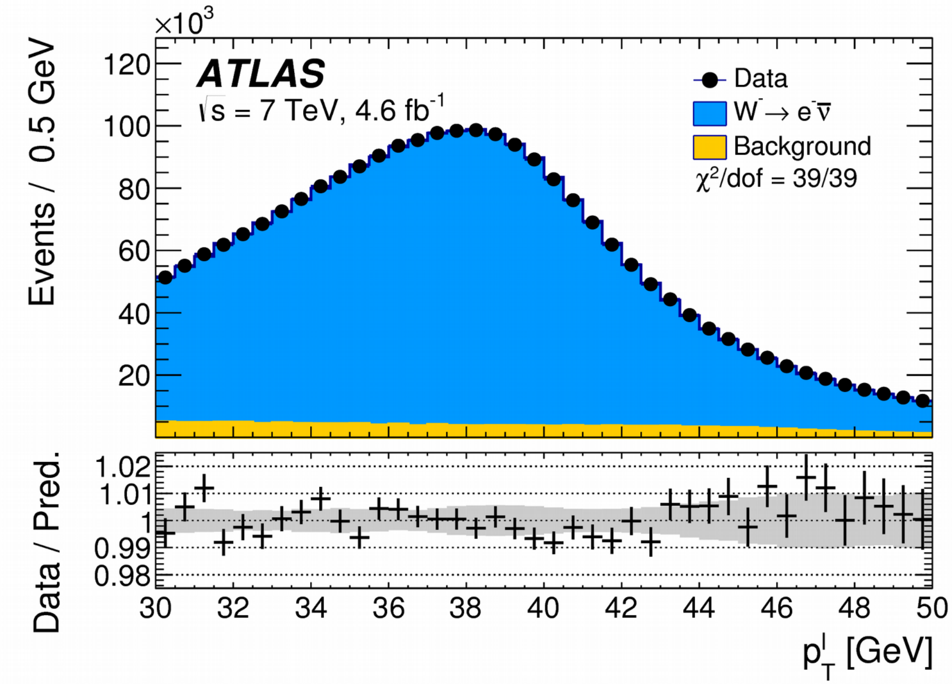

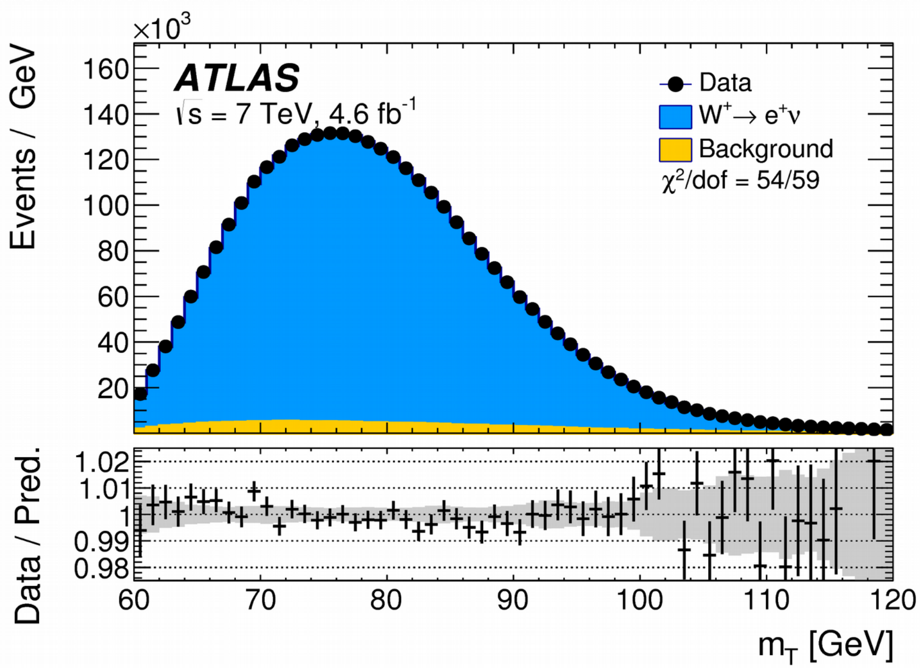

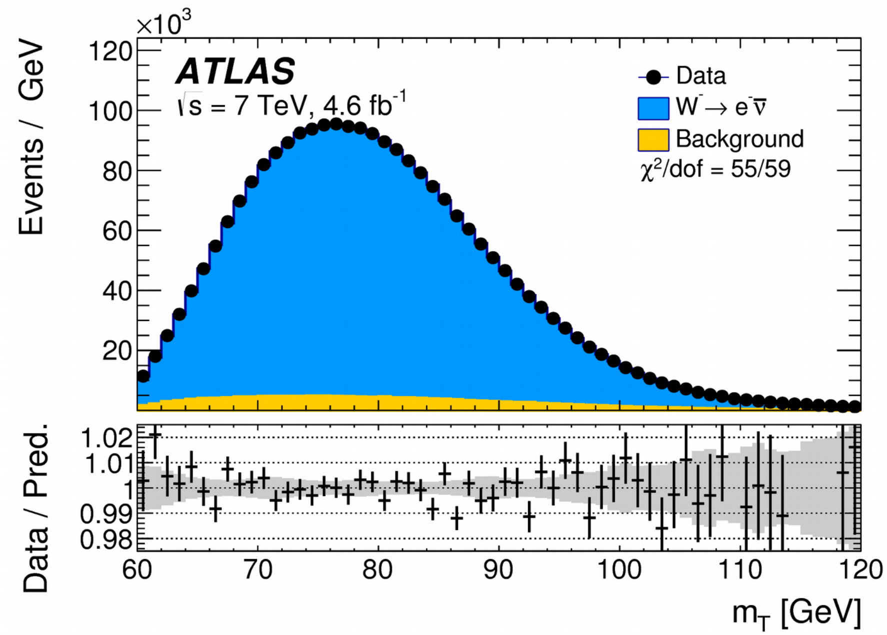

Post fit plots - muons

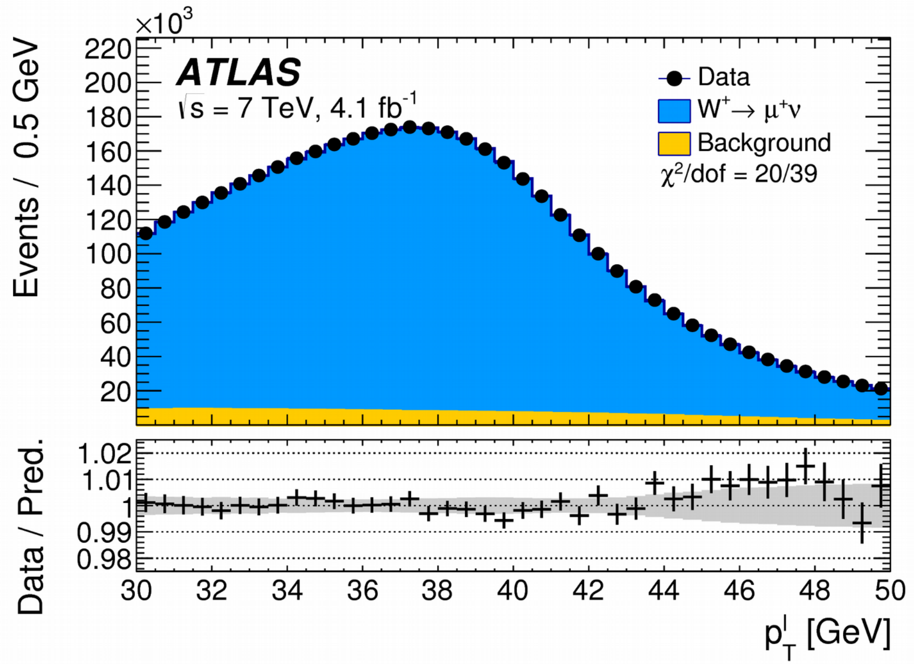

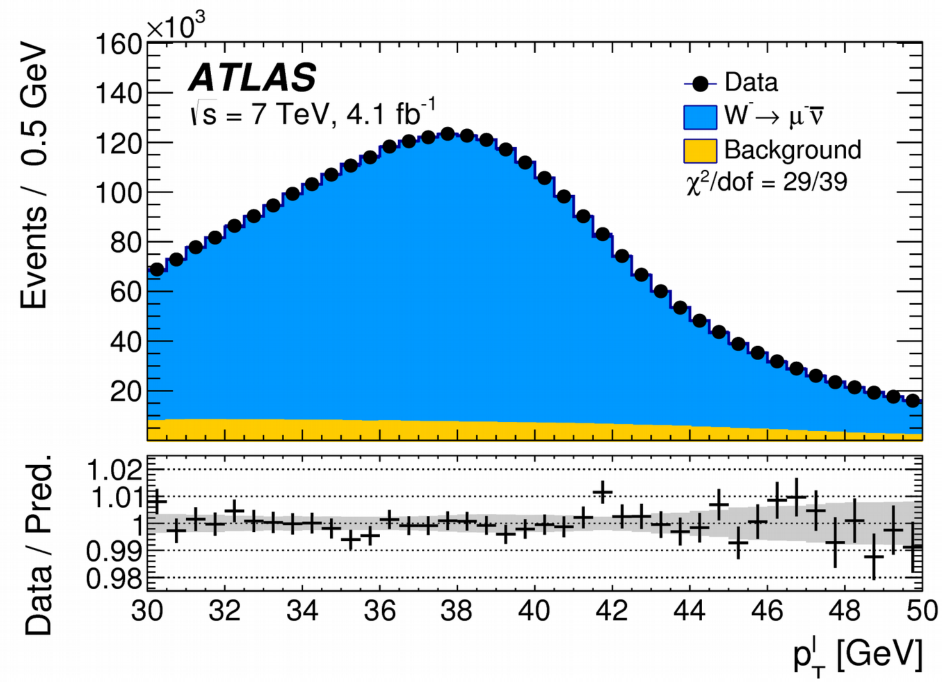

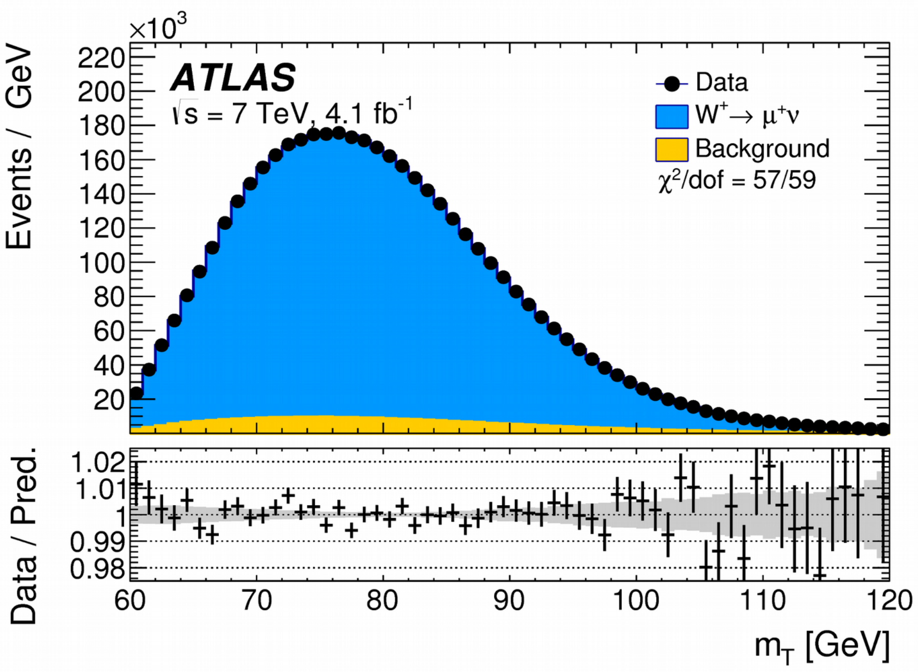

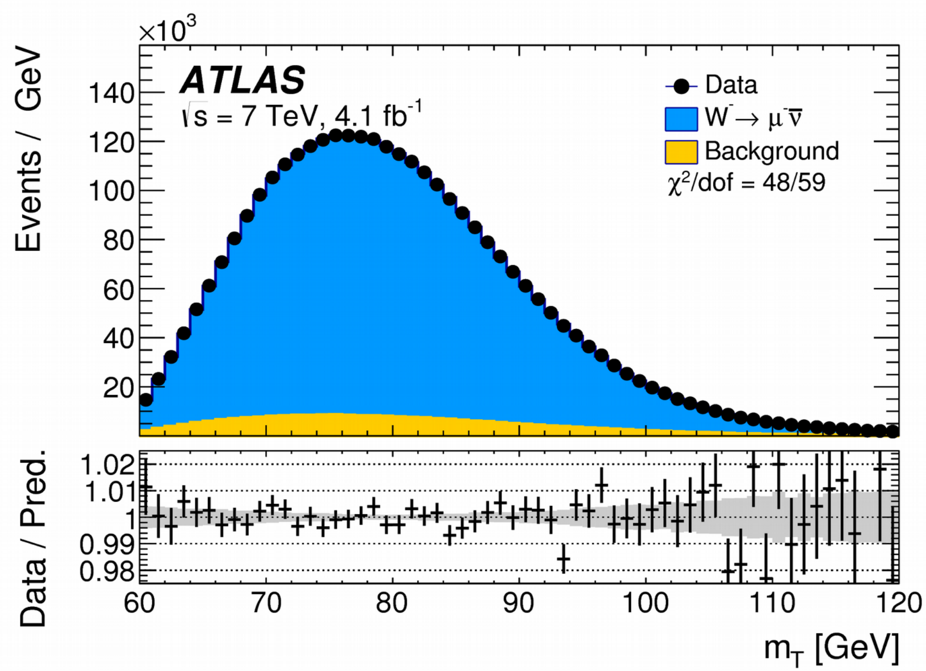

The effect of the charm mass

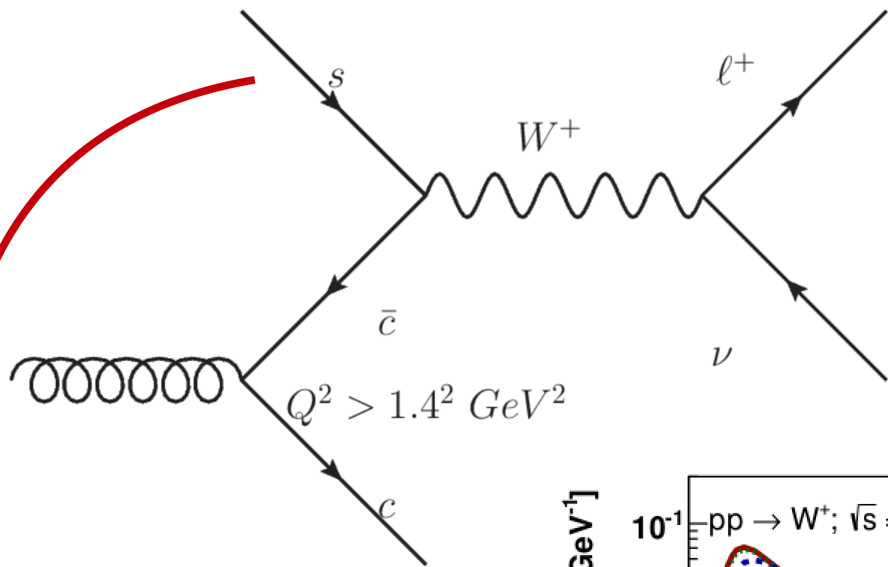

- A charm in the initial state must have come from a gluon splitting above the charm mass
- Additional recoil of about 1 GeV, harder p_T spectrum

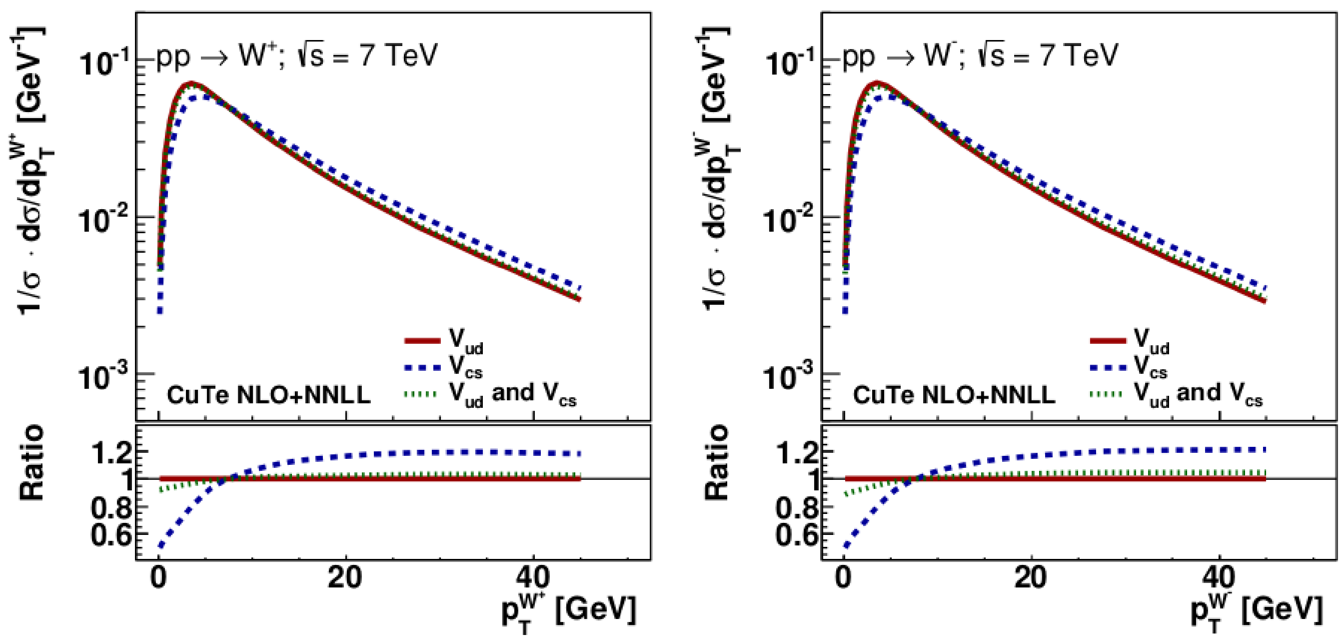

- The uncertainty on the strange PDF translates into an uncertainty on the charm-initiated W production

The effect of the charm mass

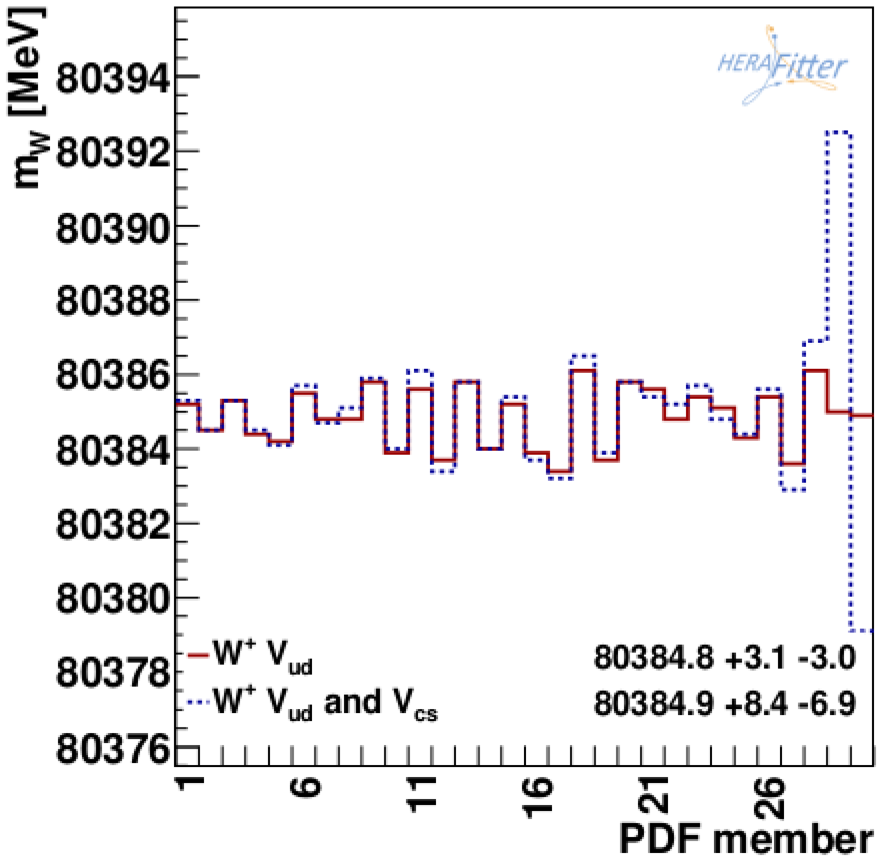

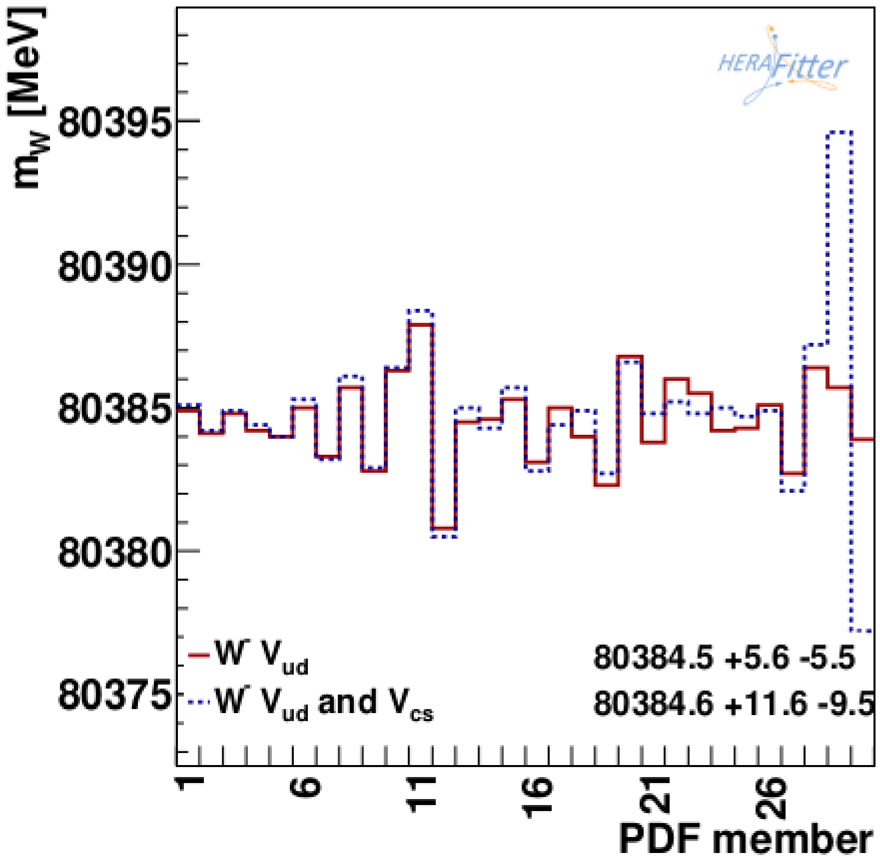

The uncertainty on the strange PDF accounts for 7-9 MeV on the W mass extracted from the lepton p_T